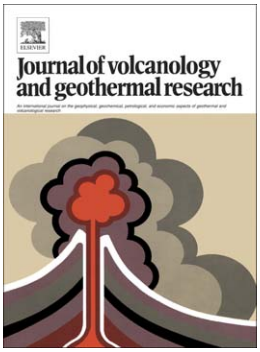

Emissions of trace elements during the 2012–2013 effusive eruption of Tolbachik volcano, Kamchatka: Enrichment factors, partition coefficients and aerosol contribution

M. Zelenski, N. Malik, Yu. Taran

PII:	S0377-0273(14)00247-9
DOI:	doi: 10.1016/j.jvolgeores.2014.08.007
Reference:	VOLGEO 5383
To appear in:	*Journal of Volcanology and Geothermal Research*
Received date:	3 April 2014
Accepted date:	2 August 2014

Please cite this article as: Zelenski, M., Malik, N., Taran, Yu., Emissions of trace elements during the 2012–2013 effusive eruption of Tolbachik volcano, Kamchatka: Enrichment factors, partition coefficients and aerosol contribution, *Journal of Volcanology and Geothermal Research* (2014), doi: 10.1016/j.jvolgeores.2014.08.007

Emissions of trace elements during the 2012-2013 effusive eruption of Tolbachik volcano, Kamchatka: enrichment factors, partition coefficients and aerosol contribution

M. Zelenski[a*], N. Malik[b], Yu. Taran[c]

a,* Corresponding author: volcangas@gmail.com; Institute of Experimental Mineralogy RAS, Chernogolovka 142432, Moscow Region, Russia; tel: +7 926 255 5948

b, Institute of Volcanology and Seismology FEB RAS, Petropavlovsk-Kamchatsky 683006, Russia

c, Institute of Geophysics, Universidad Nacional Autonoma de Mexico, Mexico D.F. 04510, Mexico

Abstract

Gases and aerosols from the 2012-13 effusive eruption of Tolbachik basaltic volcano, Kamchatka, were sampled in February and May, 2013, from a lava tube window located 300 m from the eruptive crater; temperature at the sampling point was 1060-1070^{o}C. The chemical and isotopic compositions of the sampled gases (92.4 % H_2O, 3.5% CO_2, 2.3% SO_2 on average; δD from -25.0 to -38.6‰) correspond to a typical volcanic arc gas without dilution by meteoric or hydrothermal water. Halogen contents in the gases (1.37 % HCl, 0.5 % HF) was higher than average arc values. The total amount of analyzed metallic and metalloid (trace) elements in the gas exceeded 665 ppm. Six most abundant trace elements, K (250 ppm), Na (220 ppm), Si (74 ppm), Br (48 ppm), Cu (21 ppm) and Fe (12 ppm) accounted for 95% of the total content of trace elements in the gas. The gases contained 24 ppb Re, 12 ppb Ag, 4.9 ppb Au and 0.45 ppb Pt. Refractory rock-forming elements (Mg, Al, Ca) and some other elements such as Ba and Th are transported mainly in the form of silicate microspheres and altered rock particles. The concentrations of metals in the eruptive Tolbachik gases are higher than the corresponding concentrations in high-temperature fumaroles worldwide, although the mutual ratios of the elements are approximately the same. The gas/magma partition coefficients of eleven elements exceeds unity, including the non-metals F, S, Cl, Br, As, Se and Te and the rare metals Cd, Re, Tl and Bi. Despite the relatively low concentrations of trace elements in the volcanic gases at the highest temperatures, superficial magma degassing provides information on the sources and sinks of metals.

Keywords: Tolbachik volcano; Kamchatka; eruption; gas emissions; trace elements; aerosol; partition coefficients

1. Introduction

Emissions of metals by volcanic gases has been studied for almost a century since John Shipley collected condensates and fumarolic incrustations in the Valley of Ten Thousand Smokes in 1917 (Shipley, 1920). Two years later, Allen and Zies observed in the same place the deposition of galena and sphalerite from fumarolic gases (Allen and Zies, 1923). Early studies of volcanic gases and related fumarolic deposits performed before 1959 were reviewed by White and Waring (1963). More recently, several papers have described the trace element compositions of fumarolic condensates collected around the world (e.g., Birnie and Hall, 1974; Menyailov and Nikitina, 1980; Gemmell, 1987). A subsequent period in the study of gaseous transport of trace elements began with the development of new methods to collect volcanic sublimates (Bernard and Le Guern, 1982) and thermodynamic simulations of gaseous transport and deposition of elements (e.g., Symonds et al., 1987; Quisefit et al., 1989; Symonds and Reed, 1993; Taran et al., 2001). In addition to the collection of condensates, which can be dangerous or even impossible on active volcanoes, emissions of trace elements into the atmosphere have been studied extensively using filter packs (e.g., Zoller et al., 1974; Aiuppa et al., 2003; Calabrese et al., 2011; Martin et al., 2012). The relationship between the metal content in volcanic fluids and ore deposits has also been discussed (Hedenquist and Lowenstern, 1994; Kavalieris, 1994; Williams-Jones and Heinrich, 2005). Volcanic gases transport almost the complete Periodic Table; however, most elements have extremely low concentrations (ppb-to-ppm level). The geological effects of such emissions are usually confined to the formation of fumarolic incrustations and the dissipation of element-containing aerosols in the environment. On the other hand, gas transport and deposition of elements in volcanic processes provide the opportunity to make direct observations. Therefore, despite their negligible potential for the formation of economic deposits, volcanic gases are scientifically significant as proxies for dense subterranean magmatic-hydrothermal vapors and hydrothermal fluids (Pokrovski et al., 2013).

Almost all direct sampling of volcanic gases, including those of the highest temperature gases (Taran et al., 1995; Chaplygin et al., 2012; Zelenski et al., 2013), has been performed from fumaroles. Even high-temperature fumarolic gases of 900–1000°C can be diluted by meteoric water (Taran et al., 1995; Botcharnikov et al., 2003; Chaplygin, 2009, Chaplygin et al., 2012) or can show signatures of interaction between the gas and the conduit walls (Quisefit et al., 1988; Symonds and Reed, 1993; Aiuppa et al., 2003). Undiluted and unchanged magmatic gases are rarely accessible for sampling. However, such gases are of interest in terms of their trace element compositions because they fix the gas-magma partition coefficients for different elements. Direct sampling of gases just after exsolution from a degassing magma is possible in rare cases during effusive basaltic eruptions with smooth degassing and negligible explosive activity. Only a few papers have dealt with such samples (e.g., the 1970 eruption of Kilauea; Naughton et al., 1974).

A large-scale effusive eruption from the Tolbachik volcano in Kamchatka occurred in 2012-2013 (Edwards, 2013; Volynets et al., 2013). The eruption provided opportunities to study the volatile emission of elements through repeated direct sampling of high-temperature (1060-1070°C) gas in the close proximity (2-3 m) to the degassing basaltic lava. In this paper, we present the results of direct gas sampling and filter pack sampling during the Tolbachik eruption in 2013. First, we introduce a new method for sampling volcanic gas condensates. We then characterize the major gas species and rock composition of the eruption. Then, the trace element concentrations in the gas condensates are examined, and the role of the Tolbachik aerosol in the total emissions of elements is discussed. The obtained set of gas samples contained the full spectrum of exsolved elements without losses caused by decreased temperature or dilution by meteoric water. Moderate contamination by fine fragments of magma and wall rocks was observed but was corrected for to separate the volatile emissions from the silicate and non-silicate aerosols. In the last section of the paper, we calculate the gas/magma partition coefficients.

2. Geological background

2.1. An overview of the region

Plosky (‘flat’) Tolbachik (55°49.5′ N, 160°23.5′ E, 3080 m asl) and the extinct Ostry (‘sharp’) Tolbachik (55°50.0′ N, 160°19.5′ E, 3682 m asl) form a predominantly basaltic volcanic complex in the central part of the Central Kamchatka depression, and belong to Klyuchevskoy volcanic group. This group comprises a cluster of ten extinct and five active volcanoes, at least two of which, Klyuchevskoy and Shiveluch, are among the most productive arc volcanoes on Earth (Portnyagin et al., 2005; Auer et al., 2008). Detailed geological descriptions of the region can be found in Portnyagin et al. (2007), Ponomareva et al. (2007) and Auer et al. (2008).

The Plosky Tolbachik volcano has a massive edifice with steep slopes and a flat summit that is formed by a caldera 3 km in diameter. An inner crater-caldera of 1.7 km diameter and 600 m deep is located in the southern part of the Plosky Tolbachik summit. This inner collapse crater was formed during the 1975-76 eruption of Tolbachik as a result of the emptying of the magmatic plumbing system.

Before the collapse of the caldera, a small pit crater ca. 300 m in diameter and containing an intermittent lava lake was present on the flat summit of Plosky Tolbachik. Several weak eruptions occurred from the terminal crater in the form of gas jets from the lava lake surface and sporadic explosions (Dvigalo et al., 1991). Two NE- and SSW-trending extension (‘rift’) zones with linear chains of cinder cones cross the Plosky Tolbachik edifice. Polyak and Melekestsev (1981) estimated that the average effusion rate of Tolbachik during the Holocene was 0.2 m^3/s. The last three major Tolbachik eruptions occurred in 1941, 1975-76 and 2012-13, and were located in the SSW ‘rift’ zone. The total volume of ejected lava and tephra during these three eruptions was approximately 2.0 km^3 of compact material, which corresponds to an average rate of lava production of 0.86 m^3/s for the last 72 years.

Although it is located in a subduction zone, Plosky Tolbachik exhibits several features that are characteristic of intraplate volcanoes: (1) fluid basaltic or basaltic andesite lavas with high alkali contents of up to 7% $Na_2O + K_2O$; (2) a summit caldera with a pit-crater and an intermittent lava lake (before the 1975-76 eruption); (3) rift-like lateral extension zones with numerous monogenetic cones and (4) voluminous effusive eruptions with minor explosive activity. The great depth of the upper surface of the subducting slab under the volcano (180-190 km; Gorbatov et al., 1997) also differentiates Tolbachik from most arc volcanoes. Several hypotheses have been proposed to explain the petrologic features and high effusion rates of Tolbachik and other volcanoes in the Central Kamchatka depression (Ponomareva et al., 2007; Auer et al., 2008; Nikulin et al., 2012, and references therein).

2.2. The 2012-13 Tolbachik eruption

The last Tolbachik eruption began on 27 November 2012 and lasted 270 days until 24 August 2013, but some residual activity lasted until the middle of September. The initial lava and tephra ejections occurred from several eruptive centers along a 5-km-long fissure zone on the southern flank of the Plosky Tolbachik volcano, between 55°48.1′ N, 160°20.5′ E at 2240 asl and 55°45.6′ N, 160°18.8′ E at 1500 m asl. After three days of the eruption, the activity of all but the lowermost eruptive centers ceased. The initial effusion rate was estimated to be as high as 465 m^3/s of lava during the first two days of the eruption and 140 m^3/s of lava during the next 14 days (Dvigalo et al., 2014), with simultaneous moderate tephra emissions. Later, a 120-m-high pyroclastic cone formed at the main eruptive center (Fig. 1). The average effusion rate decreased to 19 m^3/s in the middle of January 2013 and continued at this rate until early June; then the effusion rate gradually decreased until the eruption stopped. Repeated intensifications of both the strombolian activity and the effusion rate occurred during the eruption. The effusion rates and the total volume of erupted lava were calculated from direct measurements of lava volumes through photogrammetric processing of orthogonal and oblique photographs of the eruption zone (Dvigalo et al., 2014). The total volume of erupted lava and tephra was estimated at 0.60 ± 0.05 km^3.

From February through May 2013, moderate strombolian activity was ongoing at the eruptive cone (Figs. 1, 2). A lava lake approximately 20×30 m in size inside the cone was constantly agitated by gas-driven explosions, which occurred 2-10 times per minute. Lava was drained from the cone through a 1-km-long lava tube (Fig. 2) and appeared from the opening of the lava tube as surface flows. Several windows over the lava tube emitted a mixture of volcanic gases and heated atmospheric air; the latter was drawn inside the tube through several holes along the lava stream.

3. Methods

3.1. Gas sampling methods

Because of the high air content, Giggenbach bottles could not be used for the gas sampling. Instead, we pumped gas through three consecutive traps, each of which was partially filled with 30 ml of 4N KOH solution (Taran et al., 2001; Fig. 3a). The set of traps was cooled by an ice-water mixture.

A 2-3-m-long silica tube was inserted into a small hole adjacent to the side of the large window at an angle of 45° to position the tube inlet as close as possible to the lava flow. The tube inlet was located only 2-3 m above the flowing lava during the sampling session in February. The other end of the silica tube was connected through a 1-m-long flexible Teflon tube to the trap. Such a long connection was necessary because of the very hot conditions near the edge of the lava tube window. The gas was pumped using an electric pump at a flow rate of 4-5 l/min for 10-20 min for each sample. In addition to the gas samples collected in alkaline traps, gas was pumped for ~10 min through a trap filled with 30 ml of 4N KOH + 2 g $Cd(OH)_2$ to detect hydrogen sulfide.

Condensate samples were collected using the same sampling line (Fig. 3a) into two consecutive empty traps made of borosilicate glass that were cooled by snow. The time required to collect 15-20 ml of condensate varied from 5 to 20 min depending on the gas/air ratio in the lava tube.

3.2. External condensation method

A sampling method using a sequence of tubes and consecutive traps with internal condensation we will call as ‘the standard method’ (Fig. 3a). We also applied a new technique for gas condensation on the external surface of a condenser that was inserted into the gas stream (Fig. 3b); this method was called as ‘the external method’. This technique eliminate potential losses of elements inside the sampling tubes, and was especially suitable for the condensate sampling from gas-air mixture emitted from the lava tube window. The core of this system was an upside-down cone-shaped condenser made of silica glass. The condenser was internally cooled by liquid butane (boiling point of approximately 0° C). Droplets of condensate were captured in a 15 ml conical polypropylene vial, which was put into a Dewar flask for thermal insulation. Liquid butane was taken from camping gas cartridges[1]. Liquid butane is an effective substance for cooling due to its low boiling point. Because butane has a low enthalpy of vaporization, it was necessary to repeatedly refill the condenser with butane to collect an appropriate volume of condensate. Each sampling procedure continued for approximately five minutes and required about 200 ml of liquid butane (one gas cartridge). Three to four 4-5 ml samples were collected in this manner during the two sampling sessions.

3.3. Aerosol sampling and analysis

Aerosol samples were collected using 0.22 μm pore size, 25-mm-diameter Cole-Parmer cellulose acetate syringe filters and Whatman 0.2 μm PTFE membrane filters (complete filter holder devices with built-in membrane filters). Gas was pumped through the filter devices at flow rates of 5 to 20 l/min for 5-20 minutes depending on the plume density. The filters were studied under an electron microscope with EDS (Energy Dispersive Spectrometer) as unpolished samples.

3.4. Analytical methods

---

[1] Such cartridges usually contain a mixture of 80% butane or isobutane + 20% propane. The filling procedure was as follows. To decrease excess pressure, the upper part of a camping gas canister was carefully punctured with a knife above the liquid level, with precautions taken to prevent combustion. After the puncture was open, some of the propane-butane mixture boiled out, and the rest of the liquid cooled to the boiling point. The butane remaining in the canister was then handled as a low boiling temperature liquid that could easily be poured through the hole into the condenser.

A standard set of methods was used to analyze solid, liquid and gaseous samples. The gas species absorbed by the alkaline solutions were analyzed separately in the each of the three consecutive traps to control the completeness of the absorption. The total amount of absorbed gas species was then calculated for each sample. The anions F^-, Cl^-, SO_3^{2-} and SO_4^{2-} were analyzed by ion chromatography (IC) without oxidation of the analyte. In addition to the alkaline solutions, the F^- and Cl^- contents were determined using IC in acid condensates; the analyzed concentrations of F^- and Cl^- in the alkaline solutions and acid condensates were compared to assess the sampling and analytical uncertainties. The iodometric method was used to determine S^{2-} in traps with $Cd(OH)_2$. CO_2 was analyzed by the evolution volumetric method separately in aliquots from each of the consecutive traps. A saturated solution of $K_2Cr_2O_7$ in 50% H_2SO_4 was carefully added to the undiluted alkaline solution in an evacuated system; the amount of liberated gas was measured using a vacuum manometer. To ensure the complete evolution of CO_2 from the liquid, the flask with the solution was warmed to 60-70 °C and shaken. The presence of $K_2Cr_2O_7$ was necessary to oxidize the alkaline analyte containing different sulfur species. The amount of condensed water in the samples was calculated from the weight difference.

All of the condensates were analyzed by ICP-MS and ICP-AES for trace elements. The condensates were transparent liquids without colloidal sulfur or any other precipitate. A thin layer of brown precipitate consisting mainly of Fe_2O_3 and native Se was found on the walls of several polypropylene containers with the condensates; the composition of this precipitate was examined by electron microscope with EDS analysis. To dissolve this precipitate, each of the empty 15-ml containers was treated with 2 ml of aqua regia at 90° C for one hour. The aqua regia from each of the containers was then added to the corresponding condensates.

The concentrations of Si, Ti, Al, Fe, Mg, Ca, Mn, Na, K and P in the rock samples were analyzed using the X-ray Fluorescence method, F, S and Cl were determined by means of electron microprobe (EMP). Rock samples were also analyzed by ICP-MS and ICP-AES for trace elements. Before ICP analyses, the rock samples were digested using a combination of four acids (Karandashev et al., 2008). The compositions of the matrix glass and phenocrysts of the lavas were studied in polished samples under an electron microscope with a quantitative EDS analysis. Aerosols were studied directly on filters using the same electron microscope with a semi-quantitative EDS analysis (because of the unpolished surface). Additional information on the analytical conditions and equipment can be found in Appendix A.

4. Results

4.1. Rock composition

The eruptive products from the uppermost eruptive centers (ejected during the first two days) were basaltic trachyandesites (53.8-54.7 % SiO_2, 6.26-6.68 % Na_2O+K_2O; Volynets et al, 2013). The lava and tephra from the main cone, which accounted for more than 90% of the total volume of the eruption, had more mafic compositions that ranged from trachybasalts to basaltic trachyandesites (50.5-52.5 % SiO_2, 5.79-6.00 % Na_2O+K_2O). All of the lavas were enriched in TiO_2 (up to 2 %) and P_2O_5 (up to 0.8 %). The eruptive products from the 2012-13 Tolbachik eruption were more silicic and had higher contents of Zn, Cu and V than the other eruptive products at the Tolbachik volcano (Flerov et al., 1984; Portnyagin et al., 2005; Volynets et al, 2013).

The lavas contained phenocrysts of plagioclase, olivine, clinopyroxene and magnetite, with subordinate amounts of small hornblende, apatite and zircon crystals. The matrix glass contained up to 4% K_2O and 6% Na_2O. Crystals of pyrite and globules of iron and copper-iron sulfides up to 20-30 μm in diameter occurred as inclusions in olivine, magnetite and pyroxene and were rarely scattered in the matrix glass. The measured concentrations of rock-forming and trace elements in four samples of lava erupted from the main cone are listed in Supplementary Tables 3a, b (Appendix B). The average composition of the Tolbachik lava is given in Tables 1a, b. Concentrations of some of the elements in Table 1b were taken from published data for Tolbachik basalts of previous eruptions, or from published average concentrations of elements in basalts.

Table 1a. Concentrations of rock-forming oxides in the Tolbachik lava, wt. %.

Oxide	% (s.d.)
SiO_2	51.76 (0.28)
TiO_2	1.95 (0.17)
Al_2O_3	15.87 (0.15)
FeO	10.83 (0.32)
MnO	0.17 (0.006)
MgO	4.06 (0.16)
CaO	7.35 (0.14)
Na_2O	3.5 (0.10)
K_2O	2.39 (0.020)
P_2O_5	0.66 (0.013)

Values are means of 4 samples; standard deviation is given in parentheses.

Table 1b. Average concentrations of elements in the Tolbachik lava, ppm.

Element	ppm (s.d.)	Method or reference	Element	ppm (s.d.)	Method or reference
Li	17 (0.50)	ICP	Ag	0.15 (0.014)	ICP
Be	1.9 (0.0044)	ICP	Cd	0.056	ICP
B	59 (30)	(1)	In	0.11	(4)
F	660 (250)	EMP	Sn	1.9 (0.064)	ICP
Na	25700 (780)	XRF	Sb	0.47 (0.063)	ICP
Mg	24500 (940)	XRF	Te	0.004	(2,5)
Al	84000 (800)	XRF	Cs	1.9 (0.063)	ICP
Si	242000 (1300)	XRF	Ba	560 (6.9)	ICP

P	2900 (58)	XRF	La	18.8 (0.32)	ICP
S	64 (34)	EMP	Ce	51.2 (0.92)	ICP
Cl	460 (60)	EMP	Pr	7.2 (0.11)	ICP
K	19800 (170)	XRF	Nd	32.9 (1.5)	ICP
Ca	52600 (980)	XRF	Sm	7.6 (0.39)	ICP
Sc	20 (0.30)	ICP	Eu	2.0 (0.067)	ICP
Ti	11700 (990)	XRF	Gd	7.5 (0.21)	ICP
V	330 (10)	ICP	Tb	1.2 (0.030)	ICP
Cr	29 (2.8)	ICP	Dy	6.8 (0.14)	ICP
Mn	1300 (46)	XRF	Ho	1.4 (0.071)	ICP
Fe	84200 (2500)	XRF	Er	4.2 (0.13)	ICP
Co	26 (0.65)	ICP	Tm	0.57 (0.024)	ICP
Ni	34 (2.6)	ICP	Yb	3.8 (0.18)	ICP
Cu	280 (13)	ICP	Lu	0.58 (0.018)	ICP
Zn	120 (4.2)	ICP	Hf	6.8 (0.24)	ICP
Ga	18.7 (2.4)	ICP	Ta	0.52 (0.046)	ICP
Ge	1.4	(2)	W	0.91 (0.27)	ICP
As	2.1 (0.18)	ICP	Re	0.00048	(6,7)
Se	0.4 (0)	ICP	Pt	0.0041 (0.003)	(1)
Br	2.2	(3)	Au	0.0055 (0.004)	(1)
Rb	55 (0.52)	ICP	Tl	0.17 (0.079)	ICP
Sr	300 (4.9)	ICP	Pb	7.3 (0.61)	ICP
Y	36 (0.6)	ICP	Bi	0.044 (0.0060)	ICP
Zr	250 (4.6)	ICP	Th	2.7 (0.48)	ICP
Nb	6.2 (0.19)	ICP	U	1.5 (0.032)	ICP
Mo	1.9 (0.092)	ICP			

Values are means of 4 samples; standard deviation is given in parentheses. Ru, Rh, Pd, Os and Ir were below the detection limits in all of the rock samples; Hg was not analyzed. Concentrations for B, Ge, Br, Te, Re, Pt and Au were taken from literature; numbers of references are given in parentheses: 1 - Flerov et al., 1984; 2 – Wedepohl, 1995; 3 – Pineau et al., 1999; 4 – Yi et al., 1995; 5 – Yi et al., 2000; 6 – Alves et al., 2002; 7 – Dosseto et al., 2003. Also see Volynets et al. (2013).

4.2. Tolbachik eruptive gases

Three sessions of gas sampling were carried out in February, April and May 2013 during the Tolbachik eruption. Gases were collected each time at the same place from a 3 by 3 meter window (Fig. 4) over the lava tube located ~300 m south of the lava lake and 150 m from the bottom of the eruptive cone (sampling site 1 in Figs. 1 and 2).

An intense gas flux rose from the window, which consisted of a mixture of hot air and volcanic gas released from the streaming lava. Air accounted for 50-90 % of the mixture by volume, which was calculated from the molar ratio of the pumped air to collected condensate. Despite the high air content, the temperature of the gas (measured by a type-K thermocouple) was the same as the temperature of the lava (measured by a pyrometer) of 1060-1070°C. The surface of the lava flow fluctuated from 2-3 m below the edge of the window in February to 6-8 m below the edge in May.

Table 2. Chemical and isotopic compositions of the Tolbachik gas[1].

Sample or reference	Date	T,°C	Major species, mmol/mol						Water isotopes	
			H_2O	CO_2	SO_2	H_2S	HF	HCl	δD_{VSMOW} ‰	$\delta^{18}O_{VSMOW}$ ‰
2012-13 eruption	26/02/2013	1060	924.5	35.4	22.5	< dl[2]	4.2	13.3	–25	7.5
"	26/02/2013	"	944.7	23.4	14.8	"	4.3	12.8	–30.4	7.6
"	26/02/2013	"	932.0	34.3	17.1	"	4.6	12.0	–31.5	7.8
"	02/04/2013	"	933.2	35.4	9.5	"	5.7	16.2	–31.6	9.7
"	02/04/2013	"	937.3	29.2	11.1	"	6.6	15.8	–38.6	10.7
"	05/05/2013	"	891.2	48.4	40.8	"	5.1	14.5		
"	05/05/2013	"	918.9	33.6	31.5	"	4.3	11.7		
"	05/05/2013	"	908.6	38.8	34.6	"	4.8	13.1		
1975-76 eruption[3]	11/06/1976	1135	973.6	1.40	4.92	3.0	1.51	5.12	–76	9.3
"	12/06/1976	1070	990.2	3.39	1.48	0.37	0.21	2.22	–78	6.5
"	22/08/1976	1020	982.3	0.80	1.30	0.80	1.80	4.90	–72	6.5
2013 average		1060	923.8	34.8	22.7	< dl	4.95	13.7		
Arc average[4]			936.2	37.1	18.6[5]		0.61[6]	8.0		
Arc average, fumaroles[7]			945.9	24.6	13.8			6.9	–27	

[1] Accuracy of the ion chromatography method is about 5 %; accuracy for isotope measurements is 0.2 ‰ for d18O and 1 ‰ for δD. [2] The detection limit of H_2S is 0.1 mmol mol. [3] Menyailov et al. (1980). [4] From persistently degassing volcanoes (Shinohara, 2013), with the exception of HF. [5] Total sulfur. [6] Gerlach (2004). [7] Taran and Zelenski, 2014.

The gas composition of the 2012-13 Tolbachik eruption, excluding the admixture of air, is given in Table 2 along with several analyses from the 1975-76 eruption (Menyailov et al., 1980, 1984). The gas had an isotopic signature of a subduction volcano with little or no meteoric water (δD = –25.0 to –38.6, $\delta^{18}O$ = +7.5 to +10.7, typical of 'andesitic water'; Taran et al., 1989; Giggenbach, 1992). The average H_2O, CO_2 and SO_2 contents were similar to the corresponding values of the average arc gas, although Tolbachik gases were strongly enriched in HCl and HF versus 'arc averages' (Shinohara, 2013; Taran and Zelenski, 2014). Hydrogen sulfide was not detected, which can be accounted for by the initially low H_2S content and the rapid oxidation of trace amounts of H_2S by heated air before sampling.

Compared with our samples, the gases sampled by Menyailov et al. (1980, 1984) during the 1975-76 eruption were more water-rich, which could be attributed to sampling of substantially degassed lava.

This is consistent with the isotopically light hydrogen of the 1976 volcanic gas condensates (Table 2). The concentrations of HF and HCl in the 1975-76 gases were approximately the same as in the 2012-13 gases.

4.3. Trace elements in the Tolbachik emissions

4.3.1. 'Standard' versus 'external' sampling methods

A 'standard' method of condensate sampling (e.g., Menyailov et al., 1980; Chevrier and Le Guern, 1982; Quisefit et al., 1989) uses a set of sequential tubes to convey the gas to a condenser (Fig. 3a). These tubes are commonly made of silica glass and are connected to the condenser via a Teflon or silicone rubber tubing. Although this method is widely used, it has an evident drawback: trace elements from the gas can be deposited onto the inner tube walls before reaching the condenser. Moreover, low-volatile elements are more prone to deposition; therefore, the sampling procedure causes fractionation. These losses are difficult to estimate, especially in the common situation in which a series of samples is collected at a volcano using the same equipment. The deposition of elements inside the sampling line rarely attracts the attention of those who collect the gas condensates. However, researchers who have collected sublimates in silica tubes inserted into a fumarole vent (e.g., Bernard and Le Guern, 1982; Quisefit et al., 1989; Toutain and Meyer, 1989) are familiar with this phenomenon. Sublimates rapidly grow inside the sampling tube and, in the case of undiluted and hot gases, can completely block the gas flux through the tube within hours.

Condensation on an external surface can prevent the undesirable deposition of trace elements before the condenser (Fig. 3b) because of the absence of a sampling line. From thermodynamic considerations (e.g., Symonds et al., 1987; Symonds and Reed, 1993; Churakov et al., 2000; Taran et al., 2001) and experimental measurements of vapor pressures (e.g., Lamoreaux and Hildenbrand, 1984), almost all trace element species, excluding B, As and Hg but including Se and Te under oxidized conditions, have very low volatility at the temperature of water condensation (~100°C). Most species, which are initially volatile after separation from lava, form solid aerosol particles when the temperature decreases, and these particles are transported further by the gaseous phase. On the surface of an external condenser, aerosol particles are captured simultaneously with condensation of steam and acid species (e.g., Kulkarni et al, 2011). The aerosol particles then dissolve in the acidic condensate containing HF and HCl; the resulting condensate is similar to the condensate collected by the standard procedure.

The main assumption that makes the 'external' condensation method a possible alternative to the 'standard' method is that aerosols of trace elements behave as inert substances at temperatures of ~100°C and do not react with the gas during condensation (although they react with the liquid *after* condensation). In this case, no fractionation occurs between the trace elements during sampling. However, because mechanisms of aerosol deposition and vapor condensation are different, the resulting element/water ratio in the external condensates can differ from that of the gas, although the mutual ratios between the trace elements remain unchanged.

4.3.2. Variations of major species and trace elements during sampling

Two sets of condensate samples were collected on the 26 February and 5 May, 2013; each of the sets consisted of three to four 'standard' condensates and three to four 'external' condensates. On 26 February, standard condensates were collected through a 2-m-long, 20-mm-I.D. silica tube; no significant deposition inside the tube was noticed. However, on 5 May, standard condensates were collected through a 3-m-long, 15-mm-I.D. composite silica tube. The length of the tube caused cooling, which led to the deposition of abundant sublimates on the inner walls; and the corresponding condensates were significantly depleted in all elements. For this reason, we excluded from consideration three samples of standard condensates collected on 5 May. The measured concentrations of F, Cl, S and trace elements in four standard and seven external condensates are listed in Supplementary Table 4 (Appendix B). Of the 69 trace elements analyzed, 63 were measured at least in one sample. Ru, Rh, Pd, Os, Ir and Tm were below the detection limits in all of the samples; Hg was not analyzed.

In order to compare performance of the methods, and to estimate the possible deviation of the element/water ratio in the external condensates, the average element concentrations in the external (C_{ext}) and standard (C_{std}) condensates were compared on a log-log plot (Fig. 5). The external condensates were relatively enriched in almost all analyzed elements. In particular, the C_{ext}/C_{std} ratios for ten selected elements, including abundant F, Br, Na, K, Cu and Fe and rare Rb, Cs, Cd and Re, had a narrow range of 1.46–1.73 (1.6 on average). The coincidence of the C_{ext}/C_{std} ratios for the ten elements transported in different forms and with different abundances can be interpreted as a general excess of metals and metalloids in external condensates, caused by incomplete condensation of water steam during the sampling. The observed 1.6-fold excess of the listed elements corresponded to loss of ~38% of H_2O. In addition to water, approximately 27% of As, 30% of HCl and ~70% of S were lost during the external condensation. The similarity of the C_{ext}/C_{std} ratios indicates that HF and the nine selected trace elements were possibly collected completely.

Some elements had C_{ext}/C_{std} ratios higher or lower than 1.6, which could have been caused by variations of the element concentrations in the gas during successive sampling (Fig. 6). Most likely, the elements with low variations (Fig. 6a) were initially emitted in a volatile form. In contrast, the elements with high variations (Fig. 6b) were emitted as aerosol, the emissions of which could depend on the volcano dynamic, the level of the lava or the influx of air into the lava tube; all factors are quite variable. The role of aerosol in Tolbachik emissions is discussed in Sections 5.1. – 5.3.

An important issue that is visible in Fig. 5 is the enrichment by approximately one order of magnitude of the standard condensates in Si, B, Zr, Sc, Hf and U. The most probable source of this enrichment is contamination during the sampling procedure; two of the elements (Si and B) were clearly leached by HF-containing liquid from the borosilicate glass bubblers used for sampling. The origin of the other four elements is most likely the same but should be confirmed by additional experiments.

Apart from these six elements, the two methods showed the good agreement within a range of concentrations of eight orders of magnitude. This suggests that both the standard and external condensation methods were suitable for sampling. Our experience has shown, however, that only the condensates collected through a shorter and wider silica tube (2m x 20 mm I.D) were of acceptable quality. All the samples collected through a 3-m-long, 15-mm-I.D. silica tube were significantly depleted in all elements as was expected in Section 4.3.1. The depleted samples were not used in further calculations.

The external condensation method can be useful in studies of trace element emissions in the absence of fumaroles. The method can collect condensate from a gas jet emerging from a wide window, from a gas mixed with air, from a plume or even from a dense volcanic fog that is common at fumarole fields. It does not require pumping and is much faster than the widely used filter pack method. Samples collected by the external condensation demonstrate lower detection limits for trace elements in comparison with the standard method because of typically low sulfur content. Unfortunately, element-to-water ratios in the external condensates can be higher or lower then true ones depending on the sampling conditions. This disadvantage limits usability of the external method. In order to determine true concentrations of elements in the gas, the external condensates should be supplemented either by standard condensates or filter packs.

4.3.3. Average concentrations of metals and metalloids in the Tolbachik gas

On the basis of the above considerations, it is reasonable to assume that our standard condensates collected through the shorter silica tube (during the first sampling session) were correct, i.e., no significant loss of elements occurred prior to condensation. The concentrations of metals and metalloids in the Tolbachik gas were defined as the averages of four standard condensates (as measured) and seven external condensates (divided by 1.6 to reconcile the observed 1.6-fold excess of the elements). The concentrations of volatile S, F, Cl and As were taken from the standard condensates. The calculated average concentrations of trace elements in the gas are listed in Table 3. For comparison with other published data, the X/SO_2 ratios are also given.

The total amounts of metals and metalloids measured in the Tolbachik gases varied from 520 to 880 ppm. The six most abundant trace elements, on average, were K (250 ppm), Na (220 ppm), Si (74 ppm), Br (48 ppm), Cu (21 ppm) and Fe (12.4 ppm), which accounted for 95% of the total measured element content. The concentrations of the other chalcophile elements ranged from 7.6 ppm As to 0.28 ppm Te. The gases contained measureable amounts of Re (24 ppb), Ag (12 ppb), Au (4.9 ppb) and Pt (0.45 ppb), all values are average; no other PGE metals were analyzed.

The listed concentrations of trace elements, especially the alkali metals and copper, are among the highest concentrations ever measured in condensates of volcanic gases (e.g., Zelenski et al., 2013, and references therein). The basaltic composition, high temperature, high chlorine content and proximity to the surface of the degassing lava are possible factors that controlled the abundance of trace elements in the gas.

Table 3. Average concentrations of F, Cl, S and trace elements in the Tolbachik gas (ppm, ppb), X/SO_2 ratios, logarithms of enrichment factors (EF) and weight ash fractions (WAF) of elements.

Element	ppm (s.d.)	$X/SO_2 \cdot 10^6$	Log EF	WAF, %	Element	ppb (s.d.)	$X/SO_2 \cdot 10^6$	Log EF	WAF, %
S	36000 (18500)	500000	7.13	0.000007	Re	24 (4.3)	0.33	6.14	0.00007
Cl	24000 (2900)	309000	5.98	0.0001	Zr	21 (8.4)	0.29	0.37	43
F	4650 (800)	61700	5.49	0.0003	Nb	14.8 (11)	0.21	1.82	1.5
K	250 (47)	3480	2.55	0.28	Cr	14.3 (14)	0.20	1.14	7
Na	224 (49)	3110	2.37	0.43	Ag	11.6 (6.3)	0.16	3.34	0.05
Si	74 (12)	1030	0.93	12	Co	9.9 (7.1)	0.14	1.03	9
Br	48 (7.9)	667	5.79	0.00016	Ge	9.9 (0.8)	0.14	2.29	0.5
Cu	21 (3.1)	286	3.31	0.049	Sb	8.6 (2.7)	0.12	2.70	0.2
Fe	12.4 (2.7)	172	0.61	25	W	6.7 (6.9)	0.093	2.31	0.5
Al	7.9 (8.9)	110	0.42	38	Ta	6.6 (3.8)	0.092	2.55	0.3
As	7.6 (1.7)	106	5.01	0.001	Sc	6.6 (0.8)	0.091	0.96	11
Zn	4.7 (3.2)	65	3.04	0.09	Ce	5.6 (6.2)	0.077	0.48	33
Ca	4.5 (3.4)	63	0.38	42	Ni	5.5 (3.8)	0.076	0.65	22
B	1.9 (1.5)	27	2.96	0.11	Au	4.9 (2.1)	0.068	4.40	0.004
Tl	1.7 (0.4)	23	5.37	0.0004	La	2.9 (2.4)	0.040	0.63	23
Rb	1.0 (0.2)	14	2.71	0.19	Th	1.83 (1.6)	0.025	1.24	6
Mg	0.88 (0.81)	12.2	0.00	100.0	Y	1.80 (1.9)	0.025	0.15	71
Pb	0.74 (0.17)	10.3	3.47	0.03	Nd	1.28 (0.29)	0.018	0.05	89
Cd	0.66 (0.10)	9.2	5.52	0.0003	Ga	1.04 (0.03)	0.014	0.24	58
Se	0.65 (0.35)	9.0	4.66	0.002	Hf	0.87 (0.45)	0.0120	0.55	28
Bi	0.53 (0.13)	7.3	5.52	0.0003	Be	0.55 (0.09)	0.0076	0.91	12
Ti	0.44 (0.42)	6.1	0.02	95	Pt	0.45 (0.33)	0.0063	3.49	0.03
Mn	0.32 (0.20)	4.5	0.83	15	Pr	0.38 (0.35)	0.0052	0.17	68
Te	0.28 (0.10)	3.9	6.29	0.00005	Sm	0.30 (0.06)	0.0042	0.04	91
P	0.23 (0.21)	3.2	0.34	46	Yb	0.18 (0.03)	0.0025	0.12	76
Ba	0.21 (0.22)	2.9	1.01	10	Gd	0.17 (0.015)	0.0023	-0.20	
Mo	0.16 (0.043)	2.3	3.39	0.04	Dy	0.14 (0.016)	0.0019	-0.26	
Li	0.13 (0.023)	1.8	2.35	0.4	Eu	0.10 (0.02)	0.0014	0.14	72
Cs	0.102 (0.015)	1.4	3.18	0.07	Er	0.088 (0.015)	0.0012	-0.23	
Sn	0.094 (0.03)	1.3	3.14	0.07	U	0.071 (0.007)	0.0010	0.11	78
In	0.075 (0.005)	1.05	4.28	0.005	Ho	0.030 (0.003)	0.00041	-0.22	
V	0.044 (0.007)	0.61	0.57	27	Lu	0.025	0.00035	0.08	83
Sr	0.033 (0.019)	0.46	0.48	33	Tb	0.023 (0.006)	0.00033	-0.24	

Values are means of 11 samples; standard deviation is given in parentheses. For enrichment factors and weight ash fractions, see Sections 5.1. and 5.3.

5. Discussion

5.1. Enrichment factors for elements in the Tolbachik emissions

The volcanic emissions of trace elements are composed of volatile and aerosol fractions (e.g., Symonds and Reed, 1993). The volatile fraction includes elements that escape from the surface of the magma as gaseous species (they can later form condensation aerosols). Other elements leave the magma surface or conduit wall rocks as molten or solid rock particles. The enrichment factor (EF) was introduced to ascertain the contributions of the volatile and particulate fractions to the total amount of an element in a volcanic gas (Zoller et al., 1974, 1983; Lepel et al., 1978):

$$\mathrm{EF}(x) = \frac{(Cx / C_R)gas}{(Cx / C_R)rock}$$

where R is a reference element, X is an element of interest and rock is the substance that is supposed to contribute to the aerosol particles. Since the pioneering works of Zoller et al. (1974) and Lepel et al. (1978), virtually all of the studies on trace element emissions in volcanic gases have used EF in one form or another. A low-volatile and abundant element like Al (Zoller et al., 1983; Toutain et al., 1995) or Mg (Symonds et al., 1987, Taran et al., 1995; Zelenski et al., 2013) is commonly used as a reference. EFs calculated in this way range six to seven orders of magnitude, from values close to unity for the least volatile elements (Mg, Ti, Y, REE) to the highest values for elements such as S, Te and Re. The EFs for the Tolbachik condensates were calculated using Mg as a reference element because Mg is among the least volatile element and was sufficiently abundant in the condensates. The EFs are shown in Fig. 7 and listed in Table 3.

The enrichment factors for elements in the Tolbachik condensates are similar to the corresponding values for high-temperature volcanic gases discharged from other volcanoes (e.g. Symonds et al., 1987, Taran et al., 1995; Zelenski et al., 2013). The elements with the highest EFs ($>10^6$) are S, Te and Re followed by halogens and chalcophile metals. Thirty-five elements have EFs < 20; Mg, Al, Ti, Y, U and HREE had EFs ~1. Five REE elements have EFs < 1, which can be attributed to underestimations of these elements in the condensates because of their extremely low concentrations. The enrichment factors (and therefore volatilities) of the elements depend on their geochemical characteristics (Fig. 7). Chalcophile, highly siderophile elements and halogens demonstrate the highest volatilities in volcanic conditions whereas lithophile elements (with the exception of alkali metals) are among the least volatile elements. In general, the volatilities of the elements increase with increasing group number in the Periodic Table and with increasing atomic number within a group, with several exceptions. Alkali metals with anomalously high volatilities are the most notable exception to this rule.

Enrichment factors help to separate contributions of elements from two different sources, such as the volatile and ash fractions of volcanic emissions. High EFs do not necessarily imply high absolute concentrations of elements in the gas and may be misleading; for example, elements with high EFs of

~10^4–10^7 can be either abundant in the gas (S, Cl) or be associated with rare elements (Re, Pt, Au). Fig. 8 compares the absolute concentrations of elements in the Tolbachik condensates with those in the bulk average Tolbachik lava. Only eleven elements exceeded the rock values, including seven non-metals (F, Cl, Br, S, Se, Te and As) and four rare metals (Tl, Cd, Bi and Re). The concentrations of In and Au were approximately the same in the gas and lava. The absolute concentrations of most of the elements in the gas were one to four orders of magnitude lower than those in the rock. The two elements with low EFs (Si, EF = 9.5 and Fe, EF = 4.6) were among the most abundant elements in the gas because of their abundances in the rock.

5.2. Enrichments of condensates in low-volatile elements

The aerosol was the primary source of the anomalously high concentrations of low-volatile elements in the condensates. This is shown on the ternary diagram for Mg-Al-Ca, where the condensates, aerosol particles, bulk rock and matrix glass are plotted (Fig. 9). The diagram shows that the concentrations of the elements in the condensates are not proportional to their abundances in the bulk rock or silicate aerosol. The compositions of the unaltered silicate aerosol from the main crater (Supplementary Table 5a, b) were similar to the bulk rock and matrix glass. However, the altered silicate microspheres from the lava tube window (Supplementary Tables 5c) were depleted in Ca and Mg. The aerosol also contained crystals of almost pure anhydrite $CaSO_4$ (Supplementary Table 5d), aluminum fluorides (Supplementary Table 5e) and aggregates of aluminum hydroxides. The compositions of the condensates lie on a mixing line between the Al corner and an endmember that plots on the mixing line between silicate particles and anhydrite. The compositional variability of the condensates can be accounted for by the entrainment of either unaltered or altered silicate aerosols with variable amounts of anhydrite crystals and Al-rich particles. Both anhydrite and Al-rich particles could have been deposited on the lava tube walls prior to sampling, and their variability in the gas could be caused by wall erosion due to gas flow inside the lava tube.

Similar ternary diagrams for the Mg-Ti-Ba and Mg-Ti-Th systems (Fig. 10a, b) demonstrate a significant enrichment of the condensates in barium and thorium. Mg and Ti are among the least volatile elements and serve as a reference because the Ti/Mg ratio is the same for condensates and unaltered rock. The compositions of the condensates, bulk lava and unaltered silicate aerosol from the main crater show that the condensates are significantly enriched in Ba compared to the bulk rocks; a large portion of such enrichment can be associated with the dissolution of Ba-rich silicate particles and micron-size $BaSO_4$ crystals, which were observed in aerosol (Supplementary Table 5b). Similar processes could result in enrichment of condensates in Th; the possible source of the latter was tiny Th-bearing monazite crystals (Supplementary Table 5f) and Al-Fe phosphates that also were present in aerosol. For comparison, a ternary diagram for Mg-Ti-Y (Fig. 10c) shows that only minor fractionation occurred during degassing between the low-volatile trace element yttrium and the low-volatile rock-forming elements magnesium and titanium. This means that both Ti and Y can be used as refractory reference elements like Mg.

The amount of silicate aerosol in the gas can be roughly estimated from the Mg abundance in the condensates, assuming that Mg is solely transported with the silicate aerosol particles, which are completely dissolved in acid condensate:

$$\text{C}_{\text{(Si-aer)}}\text{, ppm} = C_{Mg}\left(\text{cond, ppm}\right)\times\frac{[\text{the whole rock} = 10^{6}\text{ ppm}]}{[C_{Mg}\left(\text{rock, ppm}\right)]},$$

where C_{Mg} (cond) is the concentration of Mg in the condensate, and C_{Mg} (rock) is the concentration of Mg in the rock. The calculated values of silicate aerosol in the gas ranged from 16 to 60 ppm with an average of 30 ppm.

In addition to the silicate particles, aerosol contained crystals of anhydrite $CaSO_4$ and particles of Al-rich substances, likely AlF_3 and $Al_2O_3 \cdot nH_2O$. The amounts of Ca- and Al-phases were calculated from the excess amounts of Al and Ca after subtracting the silicate fractions of these elements: $CaSO_4 \approx$ Ca (exs) × 3.4; $AlF_3 \approx$ Al (exs) × 3.1; $Al_2O_3 \approx$ Al (exs) × 1.9; all of the coefficients are derived from the corresponding formulae of the substances. The amounts of $CaSO_4$ in the gas ranged from 8 to 25 ppm, and the aluminum phases ranged from 4 to 65 ppm depending on the Al-bearing phase used for the calculations and the excess of elements. The presence in volcanic aerosol of non-silicate particles or silicate particles with the composition different from that of the rock cannot be revealed directly from the condensate composition or from calculations of enrichment factors. Additional information on the aerosol composition is required, for example, from filter packs.

5.3. Weight ash fractions of elements

Weight ash fractions, or WAFs (Aiuppa et al., 2003) directly show the contribution of silicate particles (‘ash’) to the total amount of each of the elements in volcanic gas. WAFs can be derived from the enrichment factors: WAF (%) = 1/EF·100%. Weight ash fractions range from 0 to 100%, where 100% means that an element is transported solely with the silicate aerosol. The calculated WAFs for elements in the Tolbachik gas are listed in Table 3. Similarly to enrichment factors, WAFs say nothing about the possible presence of non-silicate aerosol in the gas. We can conclude from our data that elements with WAFs higher than 50% (EF < 2) are transported mainly with fine silicate ash. This includes Mg, Ti, U, Y and REE, with the exception of La and Ce. Elements with WAFs lower than 1% (EF > 100) are emitted almost solely in the gaseous form, which includes all chalcophile and highly siderophile elements (+ Mo), halogens and alkali metals. There is also a large group of elements having 1% < WAF < 50%. This group comprises such elements as Ca, Al, Ba and Th, which were discussed earlier (Section 5.2) as elements substantially transported with non-silicate particles. The role of non-silicate aerosol can also be significant for other elements with 1% < WAF < 50% (Nb, Ta, La, Ce, etc.) but this statement cannot be proved without additional studies of aerosol.

5.4. Gas/magma partition coefficients

The gas/magma partition coefficients $K = C_{gas}/C_{magma}$ can be calculated from the concentrations of the elements in the gas samples and the composition of basaltic rock. Most of the experimental data on element (metal) partitioning are related to geologically important systems at moderate pressures and high temperatures (P = 0.1 to 2 kbar; T = ~1000 °C; see e.g., Pokrovski et al., 2013, and references therein). Few data exist for low-pressure systems such as volcanic gases.

For more accurate calculations of gas/magma partition coefficients for Tolbachik, one should use the composition of the partially degassed hot lava flow just under the gas sampling conditions, which is impossible. The known concentrations of elements in solidified basalt can be substituted for the concentrations in the hot lava. This substitution is reasonable for the majority of metals, but can result in large errors for volatile elements (S, F, Cl, Br, As, Cd, Re, Tl, Pb, Bi), which can have significantly different concentrations in the undegassed magma and in the degassed basaltic rocks. The exact values of partition coefficients for these elements can be obtained only in laboratory experiments. In the case of Tolbachik, we roughly estimated partition coefficients for volatile metals and halogens using concentrations of elements in the degassed basaltic rock samples. Partition coefficient for sulfur is unavailable because the concentration of sulfur in the partially degassed hot lava varies within two orders of magnitude.

The calculated partition coefficients for Tolbachik are shown in Fig. 11. For comparison, the partition coefficients were calculated for the high-temperature gases of the Erta Ale (1084°C) and Kudriavy (940°C) volcanoes using the data from Zelenski et al. (2013) and Taran et al. (1995), respectively. The partition coefficients C_{gas}/C_{magma} for the Tolbachik gases ranged from 75 for Te to ~0.001 for the majority of the elements. Only ten elements have C_{gas}/C_{magma} ratios >1; among them, eight have C_{gas}/C_{magma} ratios >10. Partition coefficient for sulfur is obviously higher than unity, but was not calculated.

The partition coefficients for Tolbachik are similar to those for Erta Ale. The Tolbachik gases were sampled near the degassing lava and, as a first approximation, represent gases that are in equilibrium with magma. The same is likely true for the Erta Ale gas samples. Gas samples on Erta Ale were collected from holes in a spatter cone (Zelenski et al., 2013). However, a number of signs (very high temperature of 1084 °C of the gas emissions, uneven gas flow, sounds from the underneath and high level of lava in the neighboring lava lake) evidenced that liquid lava was very high, possibly only several meters under the surface. The proximity to the degassing lava surface in both Tolbachik and Erta Ale resulted in a similar influence of secondary processes, such as aerosol entrainment from conduit walls or deposition of elements from the cooling gas.

By contrast, there is a noticeable discrepancy between the partition coefficients for Tolbachik and for Kudryavy, although a broad agreement is still visible. This discrepancy cannot be fully explained with the existing dataset. The location of the magma body at Kudryavy is unknown, but evidently magma is not located so close to the surface as in the cases of Tolbachik and Erta Ale. Conduit wall erosion could affect the trace element contents in the gas. The composition of the degassing magma at Kudryavy is not known as well. Instead, concentrations of trace elements in Quaternary basaltic andesites of the southern Kuriles were used for the calculations (Taran et al., 1995). This is different from Tolbachik and Erta Ale, where fresh solidified basaltic lava was analyzed and then this analysis was used for the calculations of the partition coefficients.

6. Conclusions

Condensates and gas samples were collected during the 2012-13 Tolbachik effusive eruption from a window over a lava tube, 300 m from the main eruption cone, which experienced persistent strombolian activity. Two complementary methods of condensate sampling were used, including a new method of condensation on the external surface of a condenser filled with liquid butane.

The high-temperature (1060°C) gases collected from the lava tube window have a subduction isotopic signature ($\delta D = -25.0$ to -38.6; $\delta^{18}O = +7.5$ to 10.7), and CO_2 and SO_2 concentrations of 3.48 and 2.27 mol % respectively, similar to the average concentrations of arc volcanoes. Gases contain much HCl (1.37 mol %) and HF (0.5 mol %), which concentrations are higher than the arc average. The H_2S content was below the detection limit because of the high temperature and high air content in the gas. The concentrations of trace elements (metals and metalloids) in the Tolbachik gases are high, up to 880 ppm in total; the average concentration is 665 ppm. The high temperature, high HCl content and the proximity of the degassing lava to the surface are three possible causes of the abundance of elements in the gas.

The silicate aerosol and altered rock aerosol are the two main factors that define the concentrations of the refractory rock-forming elements in the condensates. This included both unaltered and altered silicate particles and non-silicate particles such as crystals of $CaSO_4$, aggregates of $Al_2O_3 \cdot nH_2O$ and AlF_3, which most likely were formed during rock alteration. The gases contain an average of 30 ppm of silicate aerosol and approximately the same amount of $CaSO_4$ and aluminum compounds. The aerosol is the primary source of the high concentrations of Ba, Th, and possibly other low-volatile elements in the condensates.

The well-defined concentrations of elements in the Tolbachik gas samples and the known lava composition allow the gas/magma partition coefficients C_{gas}/C_{magma} to be calculated. These coefficients range from 75 for tellurium to < 0.001 for the majority of the refractory elements. Despite the high concentrations of the trace elements in the gas compared to other volcanoes, only seven non-metals (F, S, Cl, Br, Se, Te and As) and four rare metals (Tl, Cd, Bi and Re) had partition coefficients >1.

The 2012-13 Tolbachik eruption was a rare case where volcanic gas and condensate samples were collected in the close proximity (2 m) from the degassing lava flow and, as a first approximation, represent gases that are in equilibrium with magma. The same solidified basalt was analyzed and these analyses were used for the calculations of enrichment factors and partition coefficients. The present study expands earlier existing data on concentrations of metals and metalloids in the high-temperature volcanic gas emissions and was performed with the up-to-date equipment and methods. It is likely that the measured concentrations of trace elements in the Tolbachik gases are close to the limit of the transport capacity of volcanic gases at atmospheric pressure.

Acknowledgments

This work was possible thanks to experienced pilots from the helicopter company "Vityaz-Aero", who assisted our field work from December, 2012 through May, 2013 in the absence of roads in snow-clad Kamchatka. We thank Vasiliy Yaschuk for his logistical support. We are grateful to Vasiliy Karandashev for excellent trace element analyses, Nadia Kolotilina for ion chromatography, Natalia Kononkova for electron microprobe analyses and Aleksey Nekrasov for the outstanding help in studying our samples under the electron microscope. Constructive and thorough comments of Gleb Pokrovski and Jeff Hedenquist helped us to improve the manuscript. This work was partially supported by RFBR grant # 12-05-00936.

References

Aiuppa, A., Dongarra, G., Valenza, M., Federico, C., Pecoraino, G., 2003. Degassing of trace volatile metals during the 2001 eruption of Etna. In: Volcanism and the Earth's Atmosphere, Robock A., Oppenheimer C. (Eds.), AGU Geophysical Monograph Series 139, pp. 41–54.

Allen, E.T., Zies, E.G., 1923. A chemical study of fumaroles of the Katmai region. National Geographic Society, Contributed Technical Papers, Katmai Series 2, 75-155.

Alves, S., Schiano, P., Capmas, F., Allègre, C.J., 2002. Osmium isotope binary mixing arrays in arc volcanism. Earth and Planetary Science Letters 198, 355–369.

Auer, S., Bindeman, I., Wallace, P.J., Ponomareva, V.V., Portnyagin, M.V., 2008. The origin of hydrous, high-δ^{18}O voluminous volcanism: diverse oxygen isotope values and high magmatic water contents within the volcanic record of Klyuchevskoy volcano, Kamchatka, Russia. Contributions to Mineralogy and Petrology 157, 209–230. doi:10.1007/s00410-008-0330-0

Bernard, A., Le Guern, F., 1982. A new method for sampling and analyzing volcanic sublimates - application to Merapi volcano, Java. Journal of Volcanology and Geothermal Research 12, 133–146.

Birnie, R.W., Hall, J.H., 1974. The geochemistry of El Misti volcano, Peru fumaroles. Bulletin of Volcanology 38, 1–15.

Botcharnikov, R.E., Shmulovich, K.I., Tkachenko, S.I., Korzhinskii, M.A., Rybin, A.V., Shmulovich, K.I., 2003. Hydrogen isotope geochemistry and heat balance of a fumarolic system: Kudriavy volcano, Kuriles. Journal of Volcanology and Geothermal Research 124, 45–66. doi:10.1016/S0377-0273(03)00043-X

Calabrese, S., Aiuppa, A., Allard, P., Bagnato, E., Bellomo, S., Brusca, L., D'Alessandro, W., Parello, F., 2011. Atmospheric sources and sinks of volcanogenic elements in a basaltic volcano (Etna, Italy). Geochimica et Cosmochimica Acta 75, 7401–7425. doi:10.1016/j.gca.2011.09.040

Chaplygin, I.V., 2009. Ore Mineralization of High-Temperature Fumaroles of. Kudryavy Volcano, Iturup Island (Kurile Isles). PhD Thesis (in Russian). IGEM RAN, Moscow. 186 p.

Chaplygin, I.V., Shapar, V.N., Timofeeva, I.F., Dubinina, E.O., 2012. Direct magmatic gas sampling at Gorely volcano (Kamchatka) in 2011. Proc. EGU General Assembly. Vienna, p.13923.

Chevrier, R. M., Le Guern, F., 1982. Prélèvement et analyses des condensats de fumerolles sur volcans actifs: Soufri re de la Guadeloupe (1976-1977) et Pouzzoles et Vulcano (Italie) (1978). Bulletin of Volcanology 45, 173–178. doi:10.1007/BF02597727

Churakov, S.V., Tkachenko, S.I., Korzhinskii, M.A., Bocharnikov, R.E., Shmulovich, K.I., 2000. Evolution of composition of high-temperature fumarolic gases from Kudryavy Volcano, Iturup, Kuril Islands: the thermodynamic modeling. Geochemistry International 38, 436–451.

Dosseto, A., Bourdon, B., Joron, J.-L., and Dupre, B., 2003. U-Th-Pa-Ra study of the Kamchatka arc: New constraints on the genesis of arc lavas: Geochimica et Cosmochimica Acta 67, 2857-2877.

Dvigalo V.N., Fedotov S.A., Chirkov A.M., 1991. Plosky Tolbachik. In: Fedotov S.A. and Masurenkov Yu.P. (Eds.), Active volcanoes of Kamchatka. V. 1. Nauka, Moscow, pp. 246-273 (in Russian).

Dvigalo V.N., Svirid I.Yu., Shevchenko A.V., 2014. Photogrammetric studies of New Tolbachik Fissure eruption in 2012-2013. Proc. Annual Conf. devoted to ‘Volcanologist’s Day’, IViS DVO RAN, Petropavlovsk-Kamchatsky, pp. 58-62 (in Russian).

Edwards, B., Belousov, A., Belousova, M., Volynets, A.O., Melnikov, D.V., Chirkov, S., Demianchuk, Yu., 2013. Another “Great Tolbachik” Eruption? Eos, Transactions American Geophysical Union, 94, 189–190.

Flerov, G.B., Andreev, V.N., Budnikov, V.A., Tsyurupa, A.I., 1984. Petrology of the eruption products. In: Fedotov S.A. (Ed.) Great Tolbachik Fissure Eruption, Kamchatka, 1975–1976. Nauka, Moscow, p. 640. (in Russian).

Francis, P., Chaffin, C., Maciejewski, A., Oppenheimer, C., 1996. Remote determination of SiF_4 in volcanic plumes: a new tool for volcano monitoring. Geophysical Research Letters 23, 249–252.

Gemmell, J.B., 1987. Geochemistry of metallic trace elements in fumarolic condensates from Nicaraguan and Costa Rican volcanoes. Journal of Volcanology and Geothermal Research 33, 161–181.

Gerlach, T.M., 2004. Volcanic sources of tropospheric ozone-depleting trace gases. Geochemistry Geophysics Geosystems 5, 1–16. doi:10.1029/2004GC000747

Giggenbach, W.F., 1992. Isotopic shifts in waters from geothermal and volcanic systems along convergent plate boundaries and their origin. Earth and Planetary Science Letters 113, 495–510. doi:10.1016/0012-821X(92)90127-H

Gorbatov, A., Kostoglodov, V., Suárez, G., Gordeev, E., 1997. Seismicity and structure of the Kamchatka subduction zone. Journal of Geophysical Research 102, 17883–17898. doi:10.1029/96JB03491

Hedenquist, J.W., Lowenstern, J.B., 1994. The role of magmas in the formation of hydrothermal ore deposits. Nature 370, 519–527.

Kavalieris, I., 1994. High Au, Ag, Mo, Pb, V and W content of fumarolic deposits at Merapi volcano, central Java, Indonesia. Journal of Geochemical Exploration 50, 479–491. doi:10.1016/0375-6742(94)90037-X

Karandashev, V.K., Turanov, A.N., Orlova, T.A., Lezhnev, A.E., Nosenko, S.V., Zolotareva, N.I., Moskvitina, I.R., 2008. Use of the inductively coupled plasma mass spectrometry for element analysis of environmental objects. Inorganic Materials 44, 1491–1500.

Kulkarni, P., Baron, P.A., Willeke, K. (Eds.), 2011. Aerosol Measurement: Principles, Techniques, and Applications, 3rd edition, Wiley, NY, p. 904.

Lamoreaux, R.H., Hildenbrand, D.L., 1984. High temperature vaporization behavior of oxides. I. Alkali metal binary oxides. Journal of Physical and Chemical Reference Data 13, 151-173.

Lepel, E.A., Stefansson, K.M., Zoller, W.H., 1978. The enrichment of volatile elements in the atmosphere by volcanic activity: Augustine Volcano 1976. Journal of Geophysical Research 83, 6213–6220.

Martin, R.S., Sawyer, G.M., Day, J.A., LeBlond, J.S., Ilyinskaya, E., Oppenheimer, C., 2012. High-resolution size distributions and emission fluxes of trace elements from Masaya volcano, Nicaragua. Journal of Geophysical Research 117, 1–12. doi:10.1029/2012JB009487

Menyailov I.A. and Nikitina L.P., 1980. Chemistry and Metal Contents of Magmatic Gases: the New Tolbachik Volcanoes Case (Kamchatka). Bulletin of Volcanology 43, 197–205.

Menyailov, I.A., Nikitina, L.P., Shapar, V.N., 1980. The Geochemical features of Exhalations of Great Tolbachik Fissure Eruption, Kamchatka, 1975–1976. Nauka, Moscow, p. 236 (in Russian).

Menyailov I.A., Nikitina, L.P. Shapar, V.N., 1984. Geochemical features of volcanic gases. In: In: Fedotov S.A. (Ed.) Great Tolbachik Fissure Eruption, Kamchatka, 1975–1976. Nauka, Moscow, p. 640 (in Russian).

Mori, T., Sato, M., Shimoike, Y., Notsu, K., 2002. High SiF_4/HF ratio detected in Satsuma-Iwojima volcano’s plume by remote FT-IR observation. Earth, Planets and Space 54, 249–256.

Naughton, J.J., Lewis, V.A., Hammond, D., Nishimoto, D., 1974. The chemistry of sublimates collected directly from lava fountains at Kilauea Volcano, Hawaii. Geochimica et Cosmochimica Acta 38, 1679–1690.

Nikulin, A., Levin, V., Carr, M., Herzberg, C., West, M., 2012. Evidence for two upper mantle sources driving volcanism in Central Kamchatka. Earth and Planetary Science Letters 321-322, 14–19. doi:10.1016/j.epsl.2011.12.039

Pineau, F., Semet, M.P., Grassineau, N., Okrugin, V.M., and Javoy, M., 1999. The genesis of the stable isotope (O,H) record in arc magmas: the Kamchatka's case. Chemical Geology 135, 93-124.

Pokrovski, G.S., Borisova, A.Y., Bychkov, A.Y., 2013. Speciation and Transport of Metals and Metalloids in Geological Vapors. Reviews in Mineralogy and Geochemistry 76, 165–218. doi:10.2138/rmg.2013.76.6

Polyak, B.G. and Melekestsev, I.V., 1981. Productivity of volcanoes. Journal of Volcanology and Seismology 5, 22-37 (in Russian)

Ponomareva, V., Churikova, T., Melekestsev, I., Braitseva, O., Pevzner, M., Sulerzhitsky, L., 2007. Late Pleistocene-Holocene Volcanism on the Kamchatka Peninsula, Northwest Pacific Region. In: Volcanism and Subduction: The Kamchatka Region. J. Eichelberger, E. Gordeev, M. Kasahara, P.

Izbekov, and J. Lees (Eds.), AGU Geophysical Monograph Series 172, Washington, D.C., pp. 165-198.

Portnyagin, M.V., Hoernle, K., Avdeiko, G., Hauff, F., Werner, R., Bindeman, I., Uspensky, V., Garbe-Schönberg, D., 2005. Transition from arc to oceanic magmatism at the Kamchatka-Aleutian junction. Geology 33, 25. doi:10.1130/G20853.1

Portnyagin, M.V., Hoernle, K., Plechov, P., Mironov, N., Khubunaya, S., 2007. Constraints on mantle melting and composition and nature of slab components in volcanic arcs from volatiles (H2O, S, Cl, F) and trace elements in melt inclusions from the Kamchatka Arc. Earth and Planetary Science Letters 255, 53–69. doi:10.1016/j.epsl.2006.12.005

Quisefit, J.P., Bergametti, G., Tedesco, D., Pinart, J., Colin, J.L., 1988. Origin of particulate potassium in Mt Etna emissions before and during the 1983 eruption. Journal of Volcanology and Geothermal Research 35, 111–119. doi:10.1016/0377-0273(88)90009-1

Quisefit, J.P., Toutain, J.P., Bergametti, G., Javoy, M., Cheynet, B., Person, A., 1989. Evolution versus cooling of gaseous volcanic emissions from Momotombo Volcano, Nicaragua: Thermochemical model and observations. Geochimica et Cosmochimica Acta 53, 2591–2608. doi:10.1016/0016-7037(89)90131-2

Shinohara, H., 2013. Volatile flux from subduction zone volcanoes: Insights from a detailed evaluation of the fluxes from volcanoes in Japan. Journal of Volcanology and Geothermal Research 268, 46–63. doi:10.1016/j.jvolgeores.2013.10.007

Shipley, J.W., 1920. Some chemical observations on the volcanic emanations and incrustations in the Valley of Ten Thousand Smokes, Katmai, Alaska. American Journal of Science 50, 141–153. doi:doi:10.2475/ajs.s4-50.296.141

Symonds, R.B., Rose, W.I., Reed, M.H., Lichte, F., Finnegan, D.L., 1987. Volatilization, transport and sublimation of metallic and non-metallic elements in high temperature gases at Merapi Volcano, Indonesia. Geochimica et Cosmochimica Acta 51, 2083–2101. doi:10.1016/0016-7037(87)90258-4

Symonds, R.B., Reed, M. H., 1993. Calculation of multicomponent chemical equilibria in gas-solid-liquid systems: calculation methods, thermochemical data, and applications to studies of high-temperature volcanic gases with examples from Mount St. Helens. American Journal of Science 293, 758–864.

Taran, Yu.A., Pokrovsky, B.G., Dubik, Y.M., 1989. Isotopic composition and origin of water from andesitic magmas. Doklady Academii Nauk USSR 304, 440–443.

Taran, Y.A., Hedenquist, J.W., Korzhinskii, M., Tkachenko, S.I., Shmulovich, K.I., 1995. Geochemistry of magmatic gases from Kudryavy volcano, Iturup, Kuril Islands. Geochimica et Cosmochimica Acta 59, 1749–1761.

Taran, Y.A., Bernard, A., Gavilanes, J.-C., Lunezheva, E., Cortes, A., Armienta, M. A., 2001. Chemistry and mineralogy of high-temperature gas discharges from Colima volcano, Mexico. Implications for magmatic gas–atmosphere interaction. Journal of Volcanology and Geothermal Research 108, 245–264. doi:10.1016/S0377-0273(00)00289-4

Taran, Y., Zelenski, M., 2014. Systematics of the water isotopic composition and chlorine content in arc-volcanic gases. In: Zellmer, G. F., Edmonds, M. & Straub, S. M. (eds.) The Role of Volatiles in the Genesis, Evolution and Eruption of Arc Magmas. Geological Society, London, Special Publications, 410. http://dx.doi.org/10.1144/SP410.5

Toutain, J.P., Meyer, G., 1989. Iridium-bearing sublimates at a hot-spot volcano (Piton De La Fournaise, Indian Ocean). Geophysical Research Letters 16, 1391–1394. doi:10.1029/GL016i012p01391

Toutain, J.P., Quisefit, J.P., Briole, P., Aloupogiannis, P., Blanc, P., Robaye, G., 1995. Mineralogy and chemistry of solid aerosols emitted from Mount Etna. Geochemical Journal 29, 163–173.

Vlodavetz V.I., Naboko S.I., Piip B.I., 1963. Relations between the type of eruptions and the composition of lava as exemplified by Kamchatka and Kuriles Volcanoes. Bulletin of Volcanology 26, 100-111.

Volynets, A.O., Melnikov, D.V., Yakushev, A.I., 2013. First data on composition of the volcanic rocks of the IVS 50th anniversary Fissure Tolbachik eruption (Kamchatka). Doklady Earth Sciences 452, 953–957. doi:10.1134/S1028334X13090201

Wedepohl, K.H., 1995. The composition of the continental crust. Geochimica Cosmochimica Acta 59, 1217–1232.

White, D.E., Waring, G.A., 1963. Volcanic emanations. Washington D.C., 33 p.

Williams-Jones, A.E., Heinrich, C.A., 2005. Vapor transport of metals and the formation of magmatic-hydrothermal ore deposits. Economic Geology 100, 1287–1312.

Yi, W., Halliday, A.N., Lee, D.C., Christensen, J.N., 1995. Indium and tin in basalts, sulfides, and the mantle. Geochimica Cosmochimica Acta 59, 5081–5090.

Yi, W., Halliday, A.N., Alt, J.C., Lee, D.C., Rehkämper, M., Garcia, M.O., Langmuir C.H., Su, Y., 2000. Cadmium, indium, tin, tellurium, and sulfur in oceanic basalts: Implications for chalcophile element fractionation in the Earth. Journal of Geophysical Research 105, 18927–18948.

Zelenski, M., Fischer, T.P., de Moor, J.M., Marty, B., Zimmermann, L., Ayalew, D., Nekrasov A.N., Karandashev, V.K., 2013. Trace elements in the gas emissions from the Erta Ale volcano, Afar, Ethiopia. Chemical Geology 357, 95–116. doi:10.1016/j.chemgeo.2013.08.022

Zoller, W.H., Gladney, E.S., Duce, R. A., 1974. Atmospheric concentrations and sources of trace metals at the South pole. Science 183, 198–200. doi:10.1126/science.183.4121.198

Zoller, W.H., Parrington, J., Phelan Kotra, J., 1983. Iridium enrichment in airborne particles from Kilauea volcano: January 1983. Science 222, 4–7.

Figure captions

Fig. 1. An aerial view of the 120-m-high cinder cone of the 2012-13 Tolbachik eruption on 03/05/2013. Gas was emitted from two craters on the cone and from a lava tube window located ~300 m SW of the main crater. The numbers denote the sampling sites at the lava tube window (site 1) and at the main crater rim (site 2). Photo by Lyudmila Zemlyanskikh.

Fig. 2. A sketch showing the eruptive and degassing styles of the Tolbachik eruption. Moderate strombolian activity caused by emerging gas slugs occurred in two vents of the cinder cone. Simultaneously, a lava tube drained lava from the cone. Several windows existed in the roof of the tube, with air influx through the lower windows and strong emission of the volcanic gas - air mixture through the uppermost window. All of the condensate samples were collected from the uppermost 3-m-wide window in the roof of the lava tube (sampling site 1).

Fig. 3. Sampling scheme. **a**) Standard condensate sampling. Gas passes through a sequence of silica glass and silicone rubber or Teflon tubes and condenses inside consecutive traps usually made of borosilicate glass (‘Pyrex’); the latter are cooled by an ice-water mixture. An external pump is used to sustain the gas flux through the system. The same sampling line (**a**) was used for alkaline trap sampling, but the traps were preliminarily filled with ~30 ml of 4N KOH solution. **b**) Condensation on the external surface. A silica glass flask with a cone-shaped bottom is filled with liquid butane and inserted into the hot plume. Water steam and other condensable species condense on the outer surface of the flask and drop into a polypropylene vial, which is placed into a glass Dewar container.

Fig. 4. A glowing window in the roof of the lava tube emitting a mixture of volcanic gas and hot air. A 2-m-long silica glass sampling tube is located to the left of the window. Photo by Vasiliy Yaschuk.

Fig. 5. Concentrations of elements in condensates collected by the standard method (Fig. 3a) vs. the corresponding concentrations in condensates collected by external condensation on a cold silica cone (Fig. 3b). The average concentrations of the elements in the sample sets obtained by each of the methods were used. The comparison demonstrates a generally good agreement between the standard and external condensates, albeit with consistently higher values in the external condensate for most elements. The six elements marked by gray circles had approximately one order of magnitude higher concentrations in the standard samples; these elements were most likely extracted by acid condensates from borosilicate glass of the condensers.

Fig. 6. Relative variations of elements in collected condensates with the average concentration of each of the elements set equal to unity. **a)** Elements with low variations: alkali metals, halogens, Cu and Re; **b)** elements with high variations: Ba, Se, Nb, Al, Y, La. Sample numbers are the same as listed in Supplementary Table 4, Appendix B. Samples #1-4 are standard condensates, and samples #5-11 are external condensates. Samples #1-7 were collected on the 26 February, and samples # 8-11 were collected on the 5 May. To adjust the concentrations of the elements in the external condensates to a normal level, they were divided by 1.6 before the calculations (see text for details). Except consistently higher amount of Se and Ba in the external condensates, no significant difference is visible between the two methods or between the two sampling sessions.

Fig. 7. Logarithms of the enrichment factors for elements in the Tolbachik condensates calculated relative to magnesium content of the Tolbachik lavas. Elements with log (EF) < 0 were most likely underestimated because of low concentrations.

Fig. 8. Average concentrations of elements in condensates (mg/l) compared to the corresponding concentrations of elements in Tolbachik lavas (mg/kg). The elements are arranged from high to low concentrations in rock. The dashed line shows the hypothetical concentrations of the elements in the condensates, if they were extracted solely from the average amount of silicate aerosol in the gas (30 mg/l).

Fig. 9. Variations of Mg-Al-Ca contents in condensates and aerosols. The altered rock aerosol controls the concentrations of the refractory rock-forming elements Mg, Al and Ca in the condensates.

Fig. 10. Variations of (**a**) Ba in condensates and aerosol; (**b**) Th in condensates; and (**c**) Y in condensates. The low-volatile elements Mg and Ti serve as a reference because the Ti/Mg ratio is the same in condensates and unaltered rock.

Fig. 11. Gas/magma partition coefficients for 32 elements derived from the Tolbachik gas and lava analyses (1060°C, gray squares). For comparison, the gas/magma partition coefficients for the Erta Ale fumarolic gases (1084°C, red diamonds) and Kudryavy fumarolic gases (940°C, blue circles) are also shown. Only elements that have partition coefficients $>10^{-4}$ are included. The data are from: Tolbachik – this study; Erta Ale – Zelenski et al. (2013); Kudryavy – Taran et al. (1995).

Figure 1

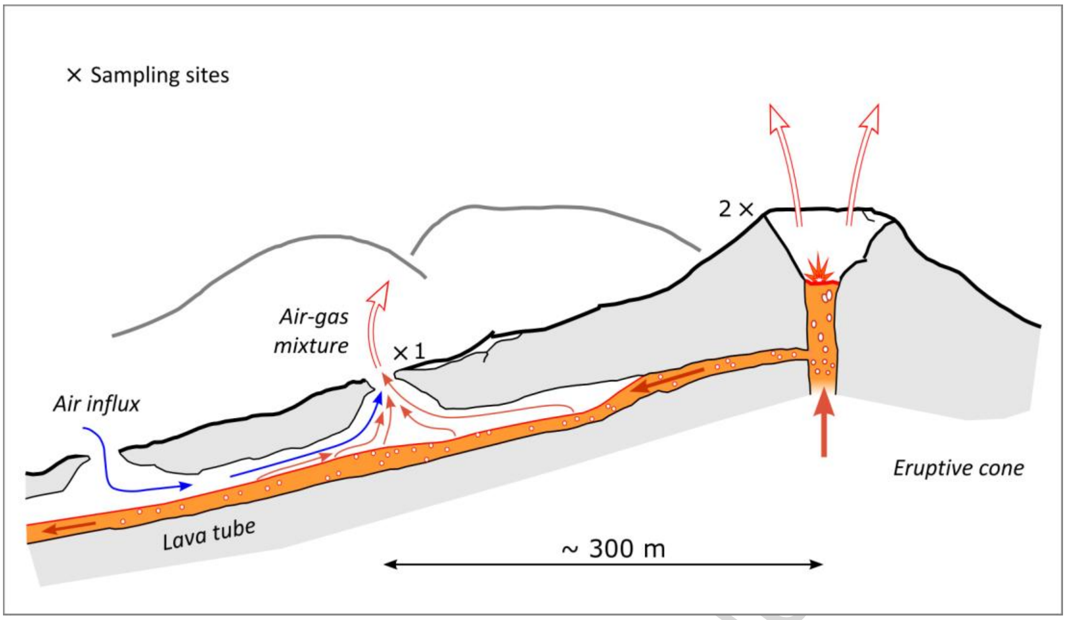
× Sampling sites
2 ×
Air-gas mixture
× 1
Air influx
Eruptive cone
Lava tube
~ 300 m

Figure 2

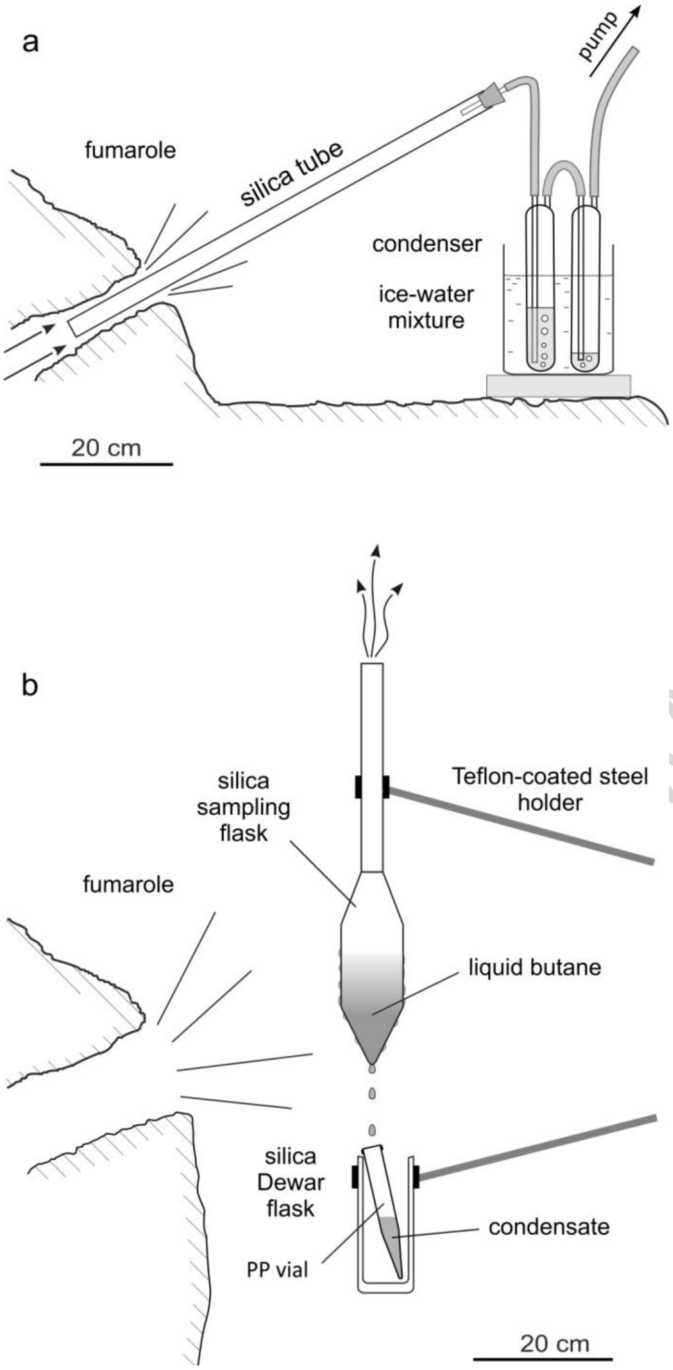
a
pump
fumarole
silica tube
condenser
ice-water mixture
20 cm
b
silica sampling flask
Teflon-coated steel holder
fumarole
liquid butane
silica Dewar flask
condensate
PP vial
20 cm

Figure 3

Figure 4

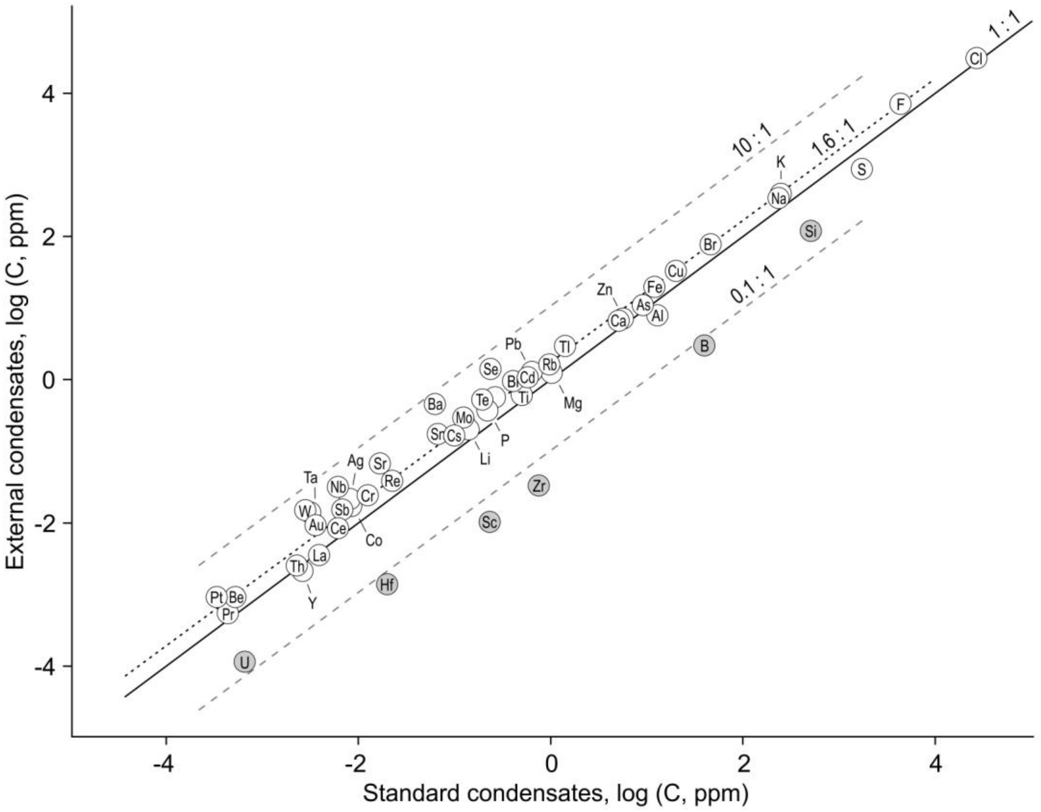
1 : 1
10 : 1
1.6 : 1
0.1 : 1
Cl
F
K
Na
S
Si
Br
Cu
Zn
Fe
As
Ca
Al
B
Pb
Tl
Se
Rb
Bi
Cd
Ti
Mg
Ba
Te
Mo
Sn
Cs
P
Li
Ag
Sr
Ta
Re
Nb
Cr
Zr
W
Sb
Au
Ce
Co
Sc
La
Th
Hf
Pt
Be
Pr
Y
U
4
2
0
-2
-4
-4
-2
0
2
4
External condensates, log (C, ppm)
Standard condensates, log (C, ppm)

Figure 5

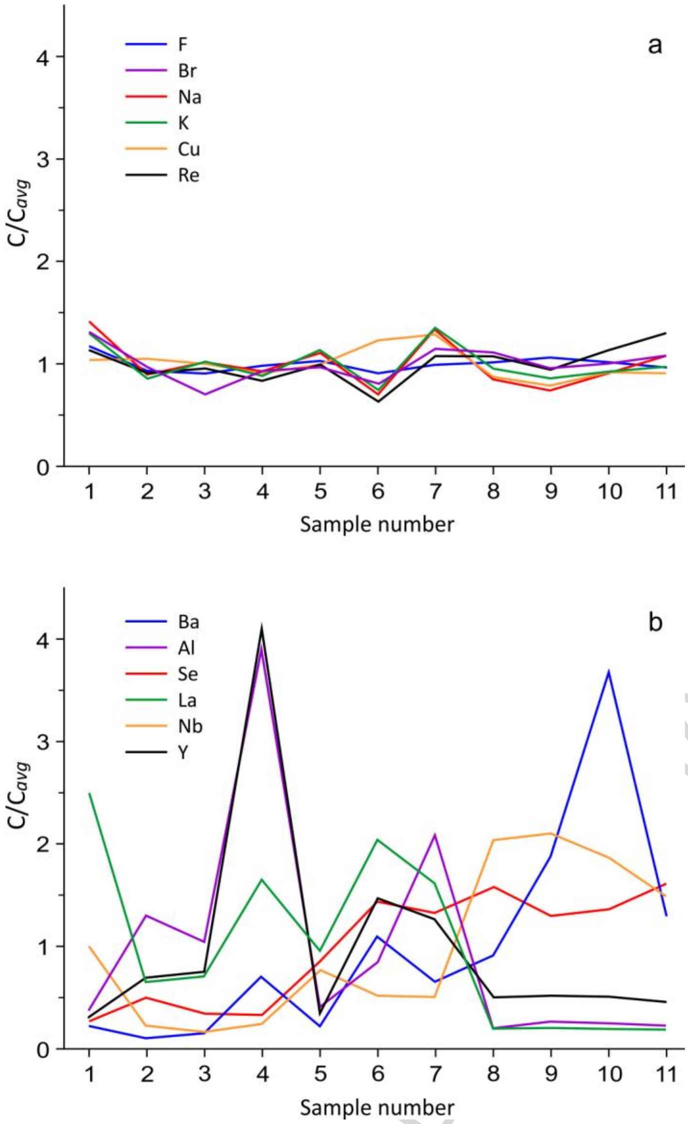
a
F
Br
Na
K
Cu
Re
C/C_{avg}
0
1
2
3
4
1
2
3
4
5
6
7
8
9
10
11
Sample number
b
Ba
Al
Se
La
Nb
Y
C/C_{avg}
0
1
2
3
4
1
2
3
4
5
6
7
8
9
10
11
Sample number

Figure 6

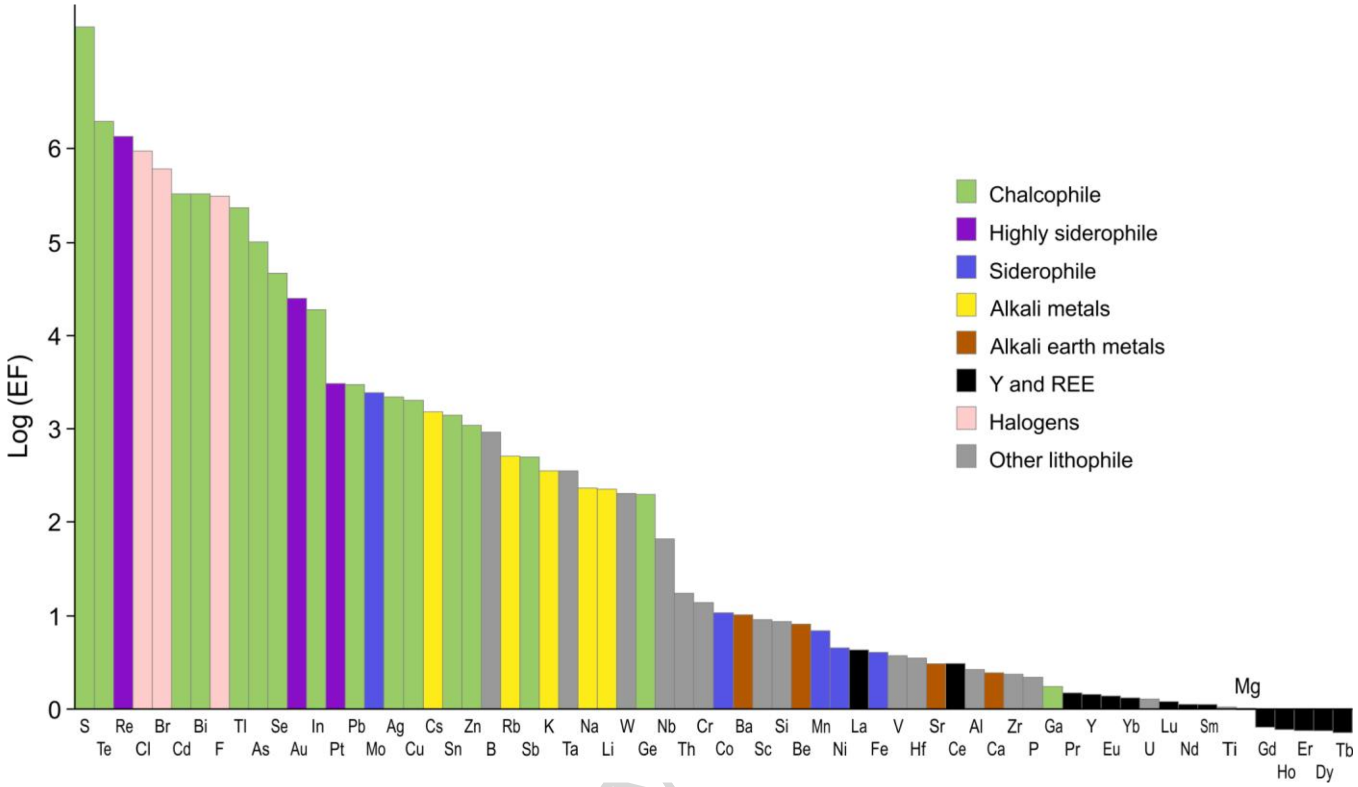
Log (EF)
0
1
2
3
4
5
6
🟩 Chalcophile
🟪 Highly siderophile
🟦 Siderophile
🟨 Alkali metals
🟫 Alkali earth metals
⬛ Y and REE
▨ Halogens
⬜ Other lithophile
Mg
S
Te
Re
Cl
Br
Cd
Bi
F
Tl
As
Se
Au
In
Pt
Pb
Mo
Ag
Cu
Cs
Sn
Zn
B
Rb
Sb
K
Ta
Na
Li
W
Ge
Nb
Th
Cr
Co
Ba
Sc
Si
Be
Mn
Ni
La
Fe
V
Hf
Sr
Ce
Al
Ca
Zr
P
Ga
Pr
Y
Eu
Yb
U
Lu
Nd
Sm
Ti
Gd
Ho
Er
Dy
Tb

Figure 7

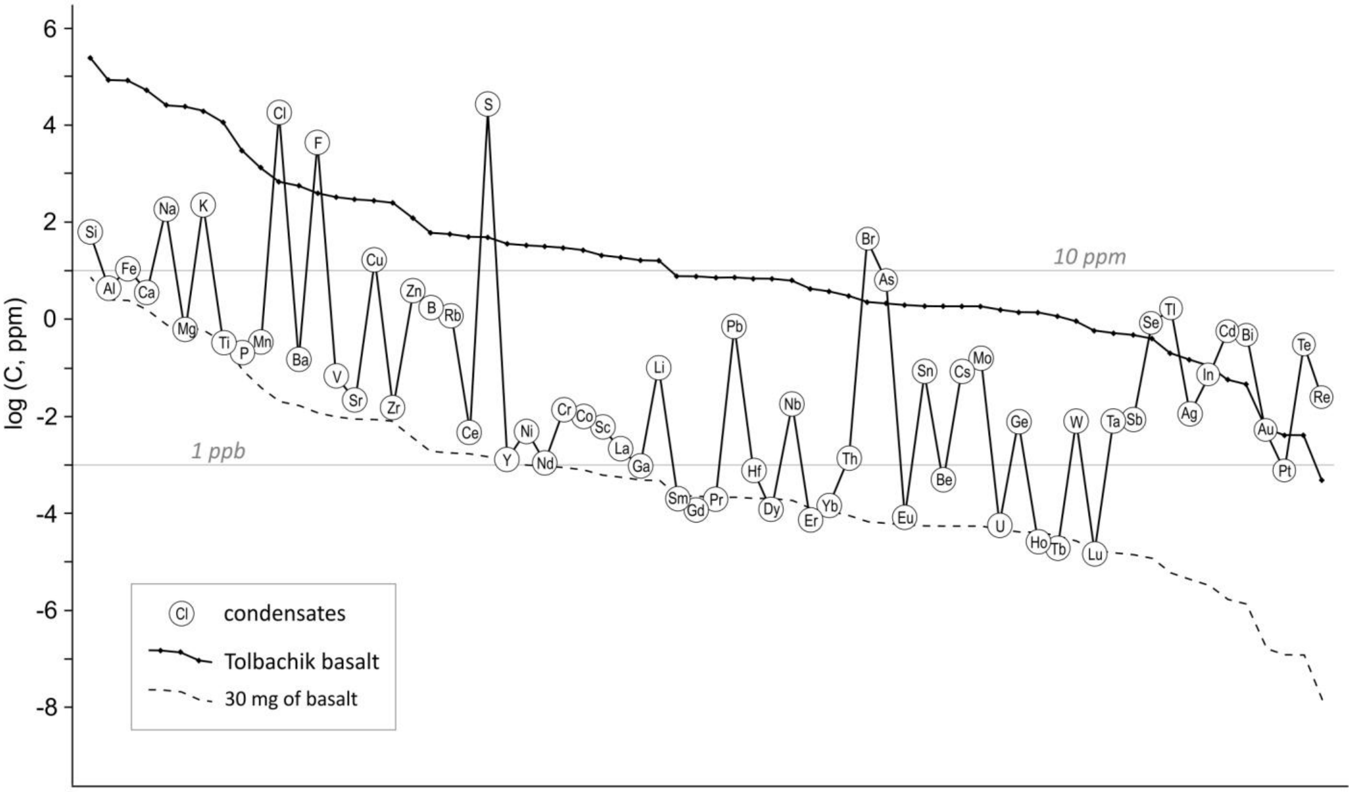
log (C, ppm)
6
4
2
0
-2
-4
-6
-8
10 ppm
1 ppb
Si
Al
Fe
Ca
Na
Mg
K
Ti
P
Mn
Cl
Ba
F
V
Sr
Cu
Zr
Zn
B
Rb
Ce
S
Y
Ni
Nd
Cr
Co
Sc
La
Ga
Li
Sm
Gd
Pr
Pb
Hf
Dy
Nb
Er
Yb
Th
Br
As
Eu
Sn
Be
Cs
Mo
U
Ge
Ho
Tb
W
Lu
Ta
Sb
Se
Tl
Ag
In
Cd
Bi
Au
Pt
Te
Re
Cl condensates
Tolbachik basalt
30 mg of basalt

Figure 8

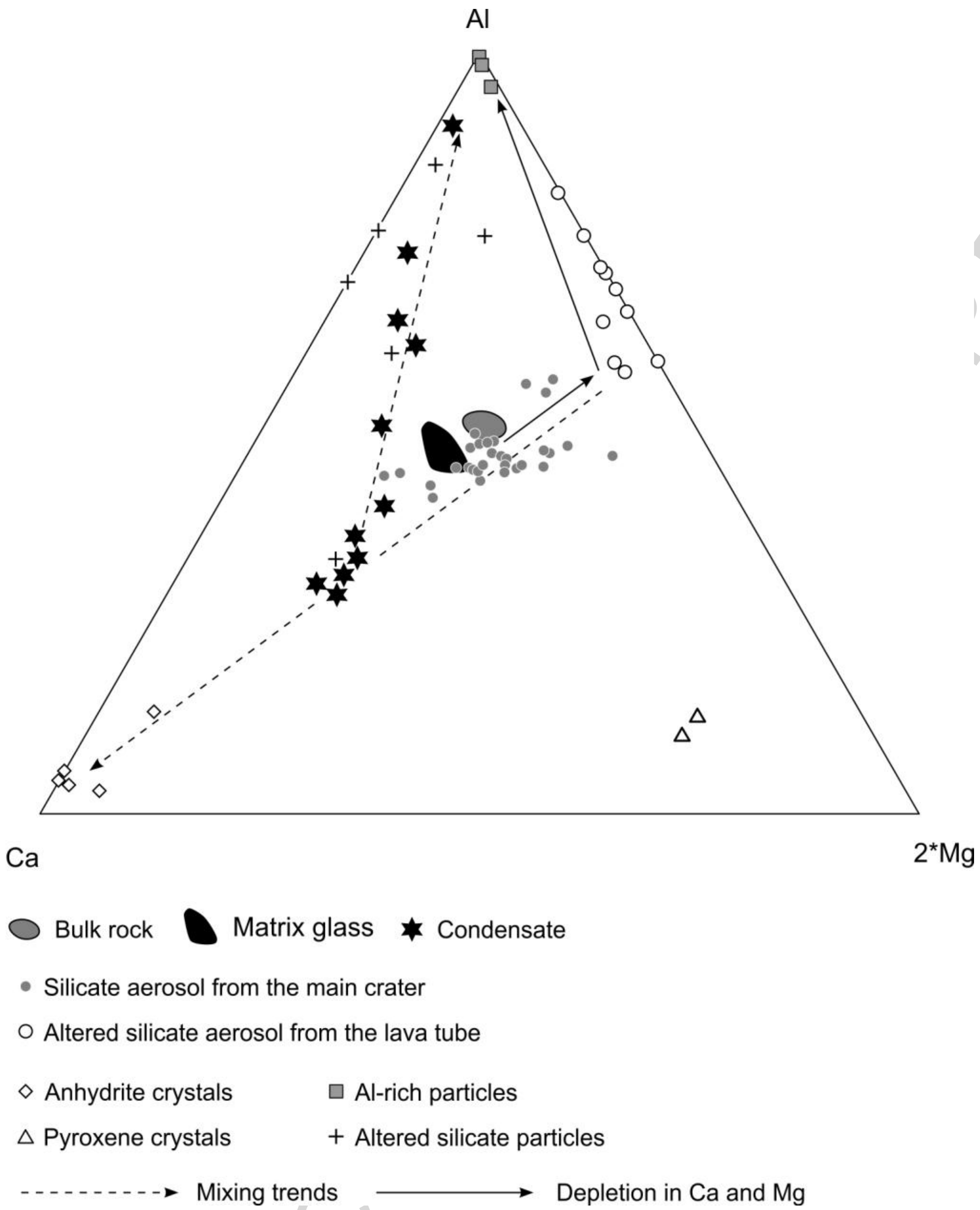
Al
Ca
2*Mg
Bulk rock
Matrix glass
Condensate
Silicate aerosol from the main crater
Altered silicate aerosol from the lava tube
Anhydrite crystals
Al-rich particles
Pyroxene crystals
Altered silicate particles
Mixing trends
Depletion in Ca and Mg

Figure 9

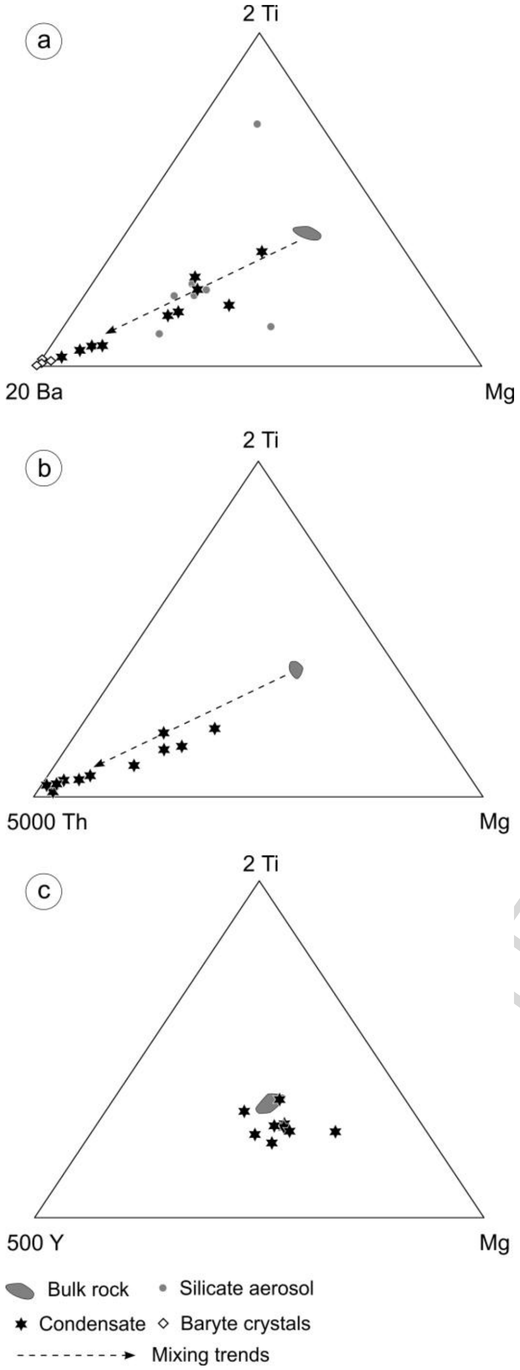
a
2 Ti
20 Ba
Mg
b
2 Ti
5000 Th
Mg
c
2 Ti
500 Y
Mg
Bulk rock
Silicate aerosol
Condensate
Baryte crystals
Mixing trends

Figure 10

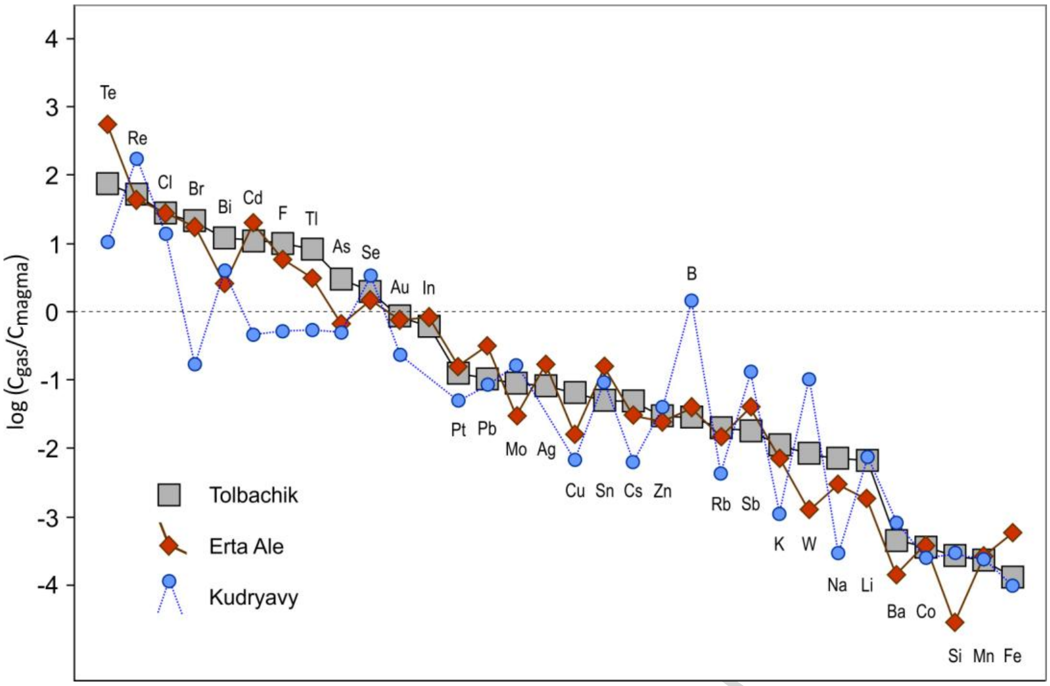
log (C_{gas}/C_{magma})
4
3
2
1
0
-1
-2
-3
-4
Te
Re
Cl
Br
Bi
Cd
F
Tl
As
Se
Au
In
Pt
Pb
Mo
Ag
Cu
Sn
Cs
Zn
B
Rb
Sb
K
W
Na
Li
Ba
Co
Si
Mn
Fe
Tolbachik
Erta Ale
Kudryavy

Figure 11

Higlights

- We sampled volcanic gas in close proximity to the degassing basaltic lava
- Concentrations of 66 major and trace elements in the gas were measured
- Aerosol was the main factor to control concentrations of low-volatile elements
- Both enrichment factors and partition coefficients for elements were calculated